Interface Reactions Responsible for Run-out in Active Brazing: Part 2

P.T. Vianco, C.A. Walker, D. De Smet,
A. Kilgo, B.M. McKenzie, and R.L. Grant

Sandia National Laboratories

Albuquerque, NM USA

Abstract

This Part 2 study examined the microstructural characteristics of braze joints made between two KovarTM base materials using the filler metals, Ag-xAl, having x = 0, 2, 5, and 10 wt.% Al additions. Brazing processes had temperatures of 965°C (1769°F) and 995°C and brazing times of 5 and 20 min. All brazing was performed under high vacuum. The objective of the present study was to build upon the findings of the Part 1, sessile drop study to identify the first-principles mechanism(s) responsible for run-out to develop a mitigation strategy to prevent this anomaly. Run-out occurs when (a) capillary flow is present and (b) the Al concentration in the filler metal is equal to, or greater than, 2 wt.%. The latter condition corresponds to the Al content exceeding 25 at.% in the reaction layer at the filler metal interface. Reaction layer cracking was observed only with the Ag-10Al filler metal and all brazing conditions. Cracking was attributed to strengthening of the filler metal that prevented the relaxation of residual stresses. The reaction layer thickness increased with Al concentration in the Ag-xAl filler metal, but largely without a statistically-significant difference as a function of brazing process parameters. This trend indicates that layer thickness, like reaction layer composition, is not dependent upon thermally-activated, rate kinetics but rather, the chemical potential (driving force) determined by the Al content. Minimizing Al content in the filler metal will mitigate run-out and prevent reaction layer cracking.

Introduction

Run-out in Ag-Cu-Zr Active Braze Joints

Run-out behavior is often attributed to an excessive quantity of filler metal introduced in the braze joint. However, another scenario for run-out was observed during the development of a braze joint between alumina ceramic and KovarTM base material using the active filler metal, 97Ag-1Cu-2Zr (wt.%, abbreviated Ag-Cu-Zr) [1, 2]. Run-out was construed to result from a localized instability in the wetting and spreading behavior of the molten filler metal. Microanalysis confirmed that Al, which is released by the reduction-oxidation ("redox") reaction between Zr and alumina, caused the run-out event when it diffused to, and then reacted with, the KovarTM base material. The early studies determined that the driving force for run-out was on-par with that of the molten filler metal surface energy. Therefore, braze joint geometry has a significant role in the run-out event.

A follow-on study documented the reaction between Al and KovarTM base material. That Part 1 investigation examined the wetting-and-spreading behavior of binary Ag-xAl filler metals, where x = 0, 2, 5, and 10 wt.%, on KovarTM base material using the *sessile drop configuration* [3]. Particular attention was given to the (Fe, Ni, Co)_xAl_y reaction layer that developed at the Ag-xAl / KovarTM base material interface. Although the run-out lobes were not observed, general wetting and spreading behavior increased significantly when the Al content in the filler metal was greater than 2 - 5 wt.%. This trend correlated to Al concentrations in the (Fe, Ni, Co)_xAl_y reaction layer that exceeded 30 - 35 at.%. The Part 1 findings also established a general insensitivity of the wetting and spreading behavior as well as reaction layer composition to the brazing temperature and time. This trend was similar to observations for the alumina / Ag-Cu-Zr / KovarTM base material system [1].

The analysis in reference 1 indicated that run-out was sensitive to the geometry of the braze joint. The run-out lobes (e.g., Fig. 1) were not observed in the sessile drop configuration.

Therefore, the current Part 2 study replaced the sessile drop configuration with a *braze joint* geometry. The braze joint, being comprised of two KovarTM base materials, introduced *capillary* forces into the wetting and spreading behavior of the Ag-xAl filler metals (x = 2, 5, and 10 wt.%).

Experimental Procedures

Base Material

Braze joint test samples were constructed using two annular flanges of Kovar[™] base material. Each flange had an outside diameter of 25.4 mm (1.00 in.); an inside diameter of 6.4 mm (0.25 in.); and thickness of 0.51 mm (0.020 in.).

Filler Metal

The starting filler metal was 100Ag. Aluminum additions were made by depositing an Al coating onto one surface of the filler metal preform using the evaporation technique. The Al layer thicknesses resulted in concentrations of 2, 5, and 10 wt.% that matched those used in the Part 1 study. Each preform had the same annular configuration as the KovarTM flanges and a thickness of 0.051 mm (0.002 in.).

Brazing Process

Duplicate test samples were fabricated under one of the four combinations of the brazing temperatures, 965°C (1769°F) or 995°C (1823°F), and brazing times, 5 min or 20 min. Brazing was performed under a high vacuum of 10⁻⁷ Torr to prevent oxidation of the Al coating. The drawback of using high vacuum was the evaporation of Ag. However, Ag evaporation was minimal in the braze joint geometry.

The braze joint was formed by placing two (2) filler metal preforms between two KovarTM flanges. The preforms were placed so that the Al coated sides faced one-another along the

centerline of the gap. This geometry required the Al to cross the molten filler metal to react with the KovarTM base material, which duplicates the conditions during the fabrication of an actual metal/ceramic braze joint.

Data Analysis

The test samples were initially inspected for run-out lobes (e.g., Fig. 1). The test samples were cross sectioned using standard metallographic techniques. The energy dispersive x-ray (EDX) analysis technique provided a qualitative assessment of elemental distributions within the braze joints. Quantitative compositions were documented for the reaction layers and remaining filler metal by electron probe microanalysis (EPMA). The latter technique used an accelerating voltage of 15 keV and a beam current of 20 nA. Data acquisition was performed in 0.5 μ m steps. However, the absolute resolution limit is $\pm 0.75 \mu$ m, or an area of 1.5 μ m diameter due to sampling volume effects at this acceleration voltage. The concentration resolutions are ± 0.1 wt.% and ± 0.5 at.% for the predominant elemental species. The traces were performed across the entire braze joint, beginning and ending a nominal distance into each of the two KovarTM base materials.

The quantitative analysis by EPMA began by determining the composition of the interface reaction layer phase(s). The reaction layer boundaries were identified by Al concentrations that had dropped to less than one atomic percent at the interfaces with the filler metal and KovarTM base material. Based upon the sessile drop data in Part 1, it was anticipated that multiple phases could develop in the interface reaction layer. Therefore, compositions were determined at three locations in the layer. Phase designations were given as low-Al (near the KovarTM base material), medium-Al at the center of the reaction layer, and high-Al at the filler metal. These analyses were performed on both reaction layers intercepted by each of three traces for a total of six data per test condition and reaction layer phase. A designated

composition was represented by the mean and an error term of plus-or-minus one standard deviation.

The EPMA technique was also used to measure the concentrations of Al, Fe, Ni, and Co in the filler metal. The concentration data were obtained at the center of the gap, away from their gradients near the interfaces.

Lastly, the reaction layer thickness was determined by placing two lines along the respective edges of the reaction layer. The distance between the lines represented the *nominal* thickness. The error term of this procedure was $\pm 0.1~\mu m$ based upon the repeatability of multiple measurements.

Results

Visual Inspection of the Test Specimens

An inspection of the sample pairs indicated only a small variability in the extent of runout between them. The run-out is illustrated in Figs. 2a – 2d for one of two samples. Each figure refers to one of the four Ag-xAl compositions: (a) 0 wt.%, (b) 2 wt.%, (c) 5 wt.%, and (d) 10 wt.%. The photographs in Fig. 2a show that run-out was absent from joints made with the Ag-0Al filler metal, regardless of brazing temperature and time duration.

Those samples using the Ag-2Al filler metal are shown in Fig. 2b. The braze joints exhibited a run-out lobe geometry. The run-out increased with brazing temperatures and time. A comparison of Figs. 2a and 2b confirmed the requirement for Al to be present for run-out to take place.

Figure 2c shows the specimens representing the Ag-5Al filler metal. Run-out was very limited for the sample brazed for 965°C (1769°F) and 5 min. But, it became more extensive across the sample edges and faces under the other three brazing conditions. In fact, this run-out exceeded the extent typically associated with metal-to-ceramic braze joints.

Lastly, the Ag-10Al filler metal experienced very widespread run-out under all brazing conditions as shown in Fig. 2d. The run-out was too extensive to discern a trend as a function of brazing temperature or time.

A comparison was made of the photographs shown in Fig. 2 with the wetting and spreading behavior of the *sessile drops* analyzed in Part 1. Run-out lobes were not observed in that prior study. Rather, an accelerated wetting and spreading behavior was observed in the range of 2 -5 wt.% Al concentration, which corroborates the appearance of run-out lobes in Fig. 2. This comparison indicates that the lobe geometry is a consequence of the joint configuration.

Microanalysis of Braze Joint Cross Sections

The Part 1 study correlated the wetting and spreading behavior to the *reaction layer composition*. The same objective was the basis of the efforts in Part 2. The Part 1 analysis did not measure the *reaction layer thickness*. The layer thickness was documented in Part 2 to (a) determine thickness versus brazing parameters and (b) identify a correlation, if any, between reaction layer thickness and composition. The physical metallurgies will be categorized according to each Ag-xAl filler metal.

Ag-0Al filler metal

These test specimens did not exhibit run-out (Fig. 2a). The Ag-0Al cross section is shown in Fig. 3 for the sample fabricated at 965°C (1769°F) and 5 min. Delamination or cracks were not observed along either interface. The EDX analysis did not identify a reaction layer at the Ag-0Al / KovarTM interface nor additional phases in the bulk filler metal. This microstructure was replicated for each of the other three brazing conditions.

The EPMA trace was taken across the interfaces and filler metal. The sample was selected, which was brazed at 995°C (1823°F) for 5 min. The representative trace is shown in

Fig. 4. A reaction layer was not discernable at either interface to within the spatial resolution limit of the EPMA technique ($\pm 0.75 \, \mu m$).

The concentrations of Fe, Ni, and Co were measured in the center portion of the filler metal field. Those values (wt.%) were Fe, 0.4±0.1; Ni, 0.20±0.04; and Co, 0.18±0.04. The value for Al, 0.047±0.008, represents the signal noise level, which is well below the ±0.1 wt.% concentration limit imposed on the data. The Fe, Ni, and Co signals were nearly an order-of-magnitude above that background level. The binary alloy phases diagrams for Ag-Co, Ag-Fe, and Ag-Ni indicate solubility limits of a few tenths of one weight percent for Fe, Ni, and Co at the brazing conditions [4]. Because phase separation was not observed in the Ag-0Al alloy, these elements existed as slightly supersaturated solutions at room temperature.

The Fe, Ni, and Co traces exhibited gradients over approximately two microns into the Ag-0Al filler metal at both interfaces. The "smearing" artifact during metallographic sample preparation was investigated as a potential source of these gradients. The assumption was made that the mechanically-removed particles would have the same composition as the KovarTM base material. The elemental fractions, Z/(Fe+Ni+Co), where Z represents Fe, Ni, or Co, were calculated, based upon their respective concentrations in the center region of the Ag-0Al filler metal. Those elemental fractions varied significantly, having the following the ranges: Fe, 0.43 – 0.53; Ni, 0.25 – 0.33; and Co, 0.16 – 0.25. By comparison, the KovarTM base material exhibited fractions of Fe, 0.54; Ni, 0.28; and Co, 0.17, which varied by *only 0.001* across the EPMA traces. Therefore, smearing was an unlikely source of either the interface gradients or Fe, Ni, and Co concentrations in the filler metal.

Ag-2Al filler metal

The Ag-2Al samples exhibited run-out that slightly increased as a function of brazing temperature and time (Fig. 2b). The braze joints exhibited reaction layers at both interfaces.

Figure 5 shows the reaction layer that formed after brazing at 965°C (1769°F) for 5 min. Neither thickness nor microstructure exhibited significant trends as a function of gap clearance. A reaction layer thickness of 2.6±0.6 μm was calculated, based on ten measurements. Recrystallization was observed in the KovarTM base material.

Shown in Fig. 6 is a higher magnification, SEM photograph of the reaction layer. The layer appeared to have a single-phase microstructure. Although the Fe-rich reaction layer was clearly visible. At this particular location, recrystallization was not observed in the KovarTM base material. Lastly, cracks were not present in the reaction layer.

The EPMA trace is shown in Fig. 7a that spans the entire joint. The cyan arrows indicate the reaction layers. The trace was amplified in Fig. 7b to show details of the left-hand side reaction layer. The Fe-rich layer was accompanied by a minimum in the Ni signal and a sharp drop-off of the Co signal. The interface reaction layers showed gradients of all Fe, Ni, Co, and Al concentrations. Three compositions were determined at the black arrows in Fig. 7, which represented the low-Al, medium-Al, and high-Al concentration points within the reaction layer. The corresponding compositions are listed, below:

- Low-Al composition: (Fe, Ni, Co)_{79±8}Al_{21±3} \approx (Fe, Ni, Co)₄Al
- Medium-Al composition: (Fe, Ni, Co)_{75±4}Al_{25±2} \approx (Fe, Ni, Co)₃Al
- High-Al composition: (Fe, Ni, Co)_{73±6}Al_{27±2} \approx (Fe, Ni, Co)₃Al

Only the low-Al and high-Al compositions were statistically different from one-another. A single composition of (Fe, Ni, Co) $_{74\pm4}$ Al $_{26\pm2}\approx$ (Fe, Ni, Co) $_3$ Al was calculated to represent the entire layer. Because the Part 1 study indicated that the Al content of the reaction layers controlled the run-out phenomenon, the individual concentrations of Fe, Ni, and Co components were not recorded and instead were combined together as a single constituent [3].

The Fe, Ni, Co, and Al concentrations were determined in the Ag-2Al filler metal to be (wt.%): Fe, 0.22±0.09; Ni, 0.13±0.06; Co, 0.12±0.04; Al, 0.073±0.010. These values were similar to those recorded in the Ag-0Al filler metal to within experimental error. The Al concentration indicates that nearly all of the original 2.0 wt.%. Al content was consumed by formation of the reaction layers.

Braze joints were also examined for the Ag-2Al filler metal and the process parameters of 965°C (1769°F) for 20 min. A statistically significant trend could not be established between reaction layer thickness and gap thicknesses. The reaction layer thickness was 3.2±0.8 μm, which is statistically similar to that measured after the five-minute brazing time. The SEM and EDX data indicated a single-phase reaction layer and only isolated regions of recrystallization in the nearby KovarTM base material. Cracks were not observed in the layers. The EPMA was not performed on these specimens, assuming a similar reaction layer structure as observed in Fig. 7.

The braze joint was examined that was fabricated at 995° C (1823° F) for 5 min. The gap clearance 1.5 ± 1.0 µm, was considerably thinner than the previous two cases. The reaction layers appeared to have a single phase and the SEM images did not show evidence of cracking in the reaction layers.

The Ag-2Al braze joint was investigated, which was fabricated at 995°C (1823°F) and 20 min. An SEM photograph is shown in Fig. 8. The reaction layer thickness was 2.7±0.5 μm and did not show a significant dependence on gap clearance. The reaction layer gray tones suggested a single-phase composition. Cracks were absent from the layers. The EDX confirmed a heighten Al signal in the adjoining KovarTM base material indicating regions of recrystallization.

Figure 9a shows an EPMA traces taken across the Ag-2Al joint [995°C (1823°F), 20 min]. The cyan arrows indicate the reaction layers. The Fe-rich layer developed at the KovarTM / reaction layer interface (red arrows), which was accompanied by a minimum in the Ni trace and a gradual decline of the Co signal.

Figure 9b is an enlarged view at the left-hand side reaction layer in Fig. 9a. The Ni and Co concentrations are relatively constant across the layer. The Al trace exhibited a slightly increasing gradient towards the filler metal that was matched by a decreasing Fe signal¹.

The EPMA confirmed the limited Al gradient in the reaction layer by similar the concentrations measured at the three black arrows in Fig. 9b:

- Low-Al composition: (Fe, Ni, Co)_{76±2}Al_{24±1} \approx (Fe, Ni, Co)₃Al
- Medium-Al composition: (Fe, Ni, Co)_{75±2}Al_{24.8±0.8} \approx (Fe, Ni, Co)₃Al
- High-Al composition: (Fe, Ni, Co)_{75±2}Al_{25±1} \approx (Fe, Ni, Co)₃Al

The concentrations were not statistically different so as to indicate separate phases. A nominal composition was calculated for the entire layer thickness to be (Fe, Ni, Co) $_{75\pm2}$ Al $_{25\pm1}\approx$ (Fe, Ni, Co) $_{3}$ Al. Whether three compositions or a single nominal composition, the Al concentrations were similar to those of the Ag-2Al reaction layers formed at 965°C (1769°F) for 5 min. However, the reduced error terms of the present case indicate that a more consistent composition was produced by the higher brazing temperature and/or longer brazing time.

Two other features are shown in Fig. 9b. First, the dashed, blue arrow indicates a roughly seven-micron wide region of Al diffusion into the KovarTM base material, which represents the recrystallization zone. The Al concentration gradient is accompanied by a similar, but smaller, gradient of the Fe signal and opposite gradients for the Ni and Co concentrations in the KovarTM base material. The trends suggest that the exchange of Ni and Co with Al promotes the recrystallization effect. The second feature is the Fe, Ni, and Co gradients that extended approximately two microns from the reaction layer / Ag-2Al interface into the filler metal.

¹ These compositional variations were below the SEM and EDX detection limits, which explains the earlier assertion that the reaction layer had a single phase.

Second phase particles were not observed in the filler metal, which implies that Fe, Ni, and Co remained in solid solution.

The Fe, Ni, Co, and Al contents were determined at the central region of the Ag-2Al filler metal field. Those concentrations (wt.%) were Fe, 0.55±0.15; Ni, 0.33±0.09; Co, 0.26±0.06; Al, 0.05±0.01. The low Al concentration confirmed its consumption through formation of the reaction layers and recrystallization zones. The Fe, Ni, and Co concentrations were more than twice those measured in the Ag-2Al filler metal when brazed at 965°C (1769°F) for 5 min, indicating that the metastable, solid-solution condition for Fe, Ni, and Co in effectively, a 100Ag filler metal, had a wide composition range.

Ag-5Al filler metal

The reaction layers were examined that were formed by the Ag-5Al filler metal after brazing at 965°C (1769°F) and 5 min. Figure 2c showed that run-out was limited to the edges of the Kovar™ flanges.

The joint microstructure is shown in Fig. 10. The reaction layer thickness was 4.9 ± 0.6 µm and independent of gap clearance. This thickness was a significant increase over that of the Ag-2Al filler metal for similar (in fact, all) process conditions. Vertical grain boundaries (blue arrows) are sites of accelerated reaction into the KovarTM base material. Multiple phases were indicated in the reaction layers by a gradient in the gray tone: darker near the filler metal and lighter towards the KovarTM base material. Cracks were not observed in either reaction layer. Lastly, second phases were absent from Ag-5Al filler metal.

The representative EPMA is shown in Fig. 11a. The red arrows identify the Fe-rich layer at the KovarTM / reaction layer interface. The reaction layer is noted by the cyan arrows. An enlarged view of the left-hand side interface is shown in Fig. 11b. The Fe peak (red arrow), which is associated with the Fe-rich reaction layer, was accompanied by a minimum in the Ni

signal and small drop-off in the Co trace. Although these trends were also observed with the Ag-2Al alloy (Figs. 7 and 9), the magnitudes were amplified in Fig. 11b.

The reaction layer in Fig. 11b exhibited a broad Al peak and an Fe signal that fluctuated, having a minimum at approximately the layer midpoint and a small peak near the reaction layer / Ag-5Al filler metal interface. The Ni signal showed a single peak, the maximum of which, coincided with the minimum in the Fe trace. The Co signal remained essentially constant across the reaction layer. Clearly, the EPMA profiles do not reflect their relative concentrations in these three elements in the Kovar™ base material. The different Fe, Ni, and Co trends imply that each element is controlled by individual driving forces (chemical potentials) present during formation of the reaction layer.

The compositions were calculated for the low-Al, medium-Al, and high-Al regions of the reaction layer identified by the three black arrows in Fig. 11b:

- Low-Al composition: (Fe, Ni, Co)_{78±8}Al_{22±3} \approx (Fe, Ni, Co)₇Al₂
- Medium-Al composition: (Fe, Ni, Co)_{69±4}Al_{31±2} \approx (Fe, Ni, Co)₇Al₃
- High-Al composition: (Fe, Ni, Co)_{59±2}Al_{41,3±0.7} \approx (Fe, Ni, Co)₃Al₂

The larger error terms reflected a greater variation of Fe, Ni, and Al concentrations across the reaction layer. The Al concentration range of $22\pm3-41.3\pm0.7$ at.% was greater than that observed with the Ag-2Al filler metal ($21\pm3-27\pm2$ at.%) for the same brazing conditions.

The dashed blue arrow identified the Al diffusion gradient that extended nearly five microns into the KovarTM base material. This gradient was indicative of recrystallization.

Iron, Ni, and Co exhibited gradients that extended approximately $2-3~\mu m$ into the filler metal from the reaction layer / Ag-5Al interface (Fig. 11b). The SEM images did not resolve second phases in that region. The Al gradient was considerably steeper and approached the

spatial resolution limit of the EPMA, which implies that there was a relatively sharp termination to the reaction layer.

The Fe, Ni, Co, and Al concentrations were recorded in the center portion of Ag-5Al filler metal field (wt.%): Fe, 0.30±0.05; Ni, 0.17±0.05; Co, 0.15±0.03; Al, 1.83±0.14. The Fe, Ni, and Co levels were statistically similar to those measured with the Ag-2Al filler metal after brazing at 965°C (1769°F) for 5 min. However, the Al concentration was significantly higher at 1.83±0.14 wt.%. Clearly, the Al was not fully consumed by the reaction layer formation. The Ag-Al binary alloy phase diagram indicated that this quantity of Al should remain in complete solid solution within the Ag matrix down to 25°C (77°F) [5]. This stipulation was confirmed by the absence of identifiable second phase structures in the filler metal.

Scanning electron microscope photographs were examined of Ag-5Al braze joints fabricated at 965°C (1769°F) and 20 min as well as 995°C (1823°F) and 5 min. Figure 2c showed both cases to have experienced extensive run-out. The longer brazing time and/or higher brazing temperature did not generate observable changes to the reaction layer, the filler metal, or the KovarTM base material microstructures. A few scattered pores were observed in the reaction layers. The reaction layer thicknesses were $4.7\pm0.8~\mu m$ [965°C (1769°F) and 20 min] and $4.8\pm0.4~\mu m$ [995°C (1769°F) and 5 min]. These thickness values were not a function of gap clearance and were statistically the same as $4.9\pm0.6~\mu m$ that was measured after brazing at 965°C (1769°F) and 5 min. Cracks were absent from the layers.

The SEM micrograph in Fig. 12 shows the braze joint formed by the Ag-5Al filler metal when the brazing conditions were 995°C (1769°F) and 20 min. Run-out was very extensive as shown in Fig. 2c. Although the gap clearance varied from 6.4 μm to 28.2 μm, the reaction layer thickness was relatively constant with a value of 5.5±0.6 μm. Vertical grain boundaries were observed in the layers. Cracks were absent. The Fe-rich reaction layer was prominent at the

reaction layer / KovarTM base material interface as was recrystallization in the KovarTM base material.

The representative EPMA plot is shown in Fig. 13a. The reaction layers are clearly identified by the broad Al peak. The red arrows locate the Fe-rich layer between the reaction layer and KovarTM base material. The details of the interface microstructure are shown by the expanded EPMA plot in Fig. 13b. The Fe-rich phase (red arrow) was accompanied by a minimum in the Ni concentration and drop off of the Co signal. The dashed, blue arrow shows the extensive diffusion of Al into the KovarTM base material responsible for the recrystallization zone. That Al gradient in the recrystallization zone was accompanied by a similar gradient in the Fe concentration as well as opposite gradients of both Ni and, to a lesser degree, Co.

Both Al and Ni showed maxima in the reaction layer (Fig. 13b). The Fe concentration gradually decreased to a minimum just before the reaction layer / filler metal interface. An additional Fe peak was not present at that interface as was observed when the brazing conditions were 965°C (1769°F) and 5 min (Fig. 11b). The Co signal remained largely constant in the reaction layer. Lastly, Fe, Ni, and Co exhibited gradients of decreasing concentration approximately 2 – 3 µm into the Ag-5Al filler metal beyond the reaction layer.

The EPMA graph (Fig. 13b) shows the three black arrows that identify the locations where the determination was made of the low-Al, medium-Al, and high-Al phase compositions listed below:

- Low-Al composition: (Fe, Ni, Co)_{80±2}Al_{20.3±0.7} \approx (Fe, Ni, Co)₄Al
- Medium-Al composition: (Fe, Ni, Co)_{74±2}Al_{26±1} \approx (Fe, Ni, Co)₃Al
- High-Al composition: (Fe, Ni, Co)_{70±2}Al_{30±1} \approx (Fe, Ni, Co)₇Al₃

These compositions were compared to those measured in reaction layers created under the brazing conditions of 965°C (1769°F) and 5 min. The low-Al composition, which developed closest to the Kovar[™] base material, was nearly the same. On the other hand, the medium-Al and high-Al compositions had significantly *lower* Al concentrations after brazing at 995°C (1769°F) for 20 min versus the 965°C (1769°F), 5 min conditions. Moreover, nearly all of the Al content was consumed from the filler metal under the 995°C (1769°F) and 20 min conditions. Figures 11a and 11b indicated that 1.83±0.14 wt.% of Al remained in the filler metal.

Together, the Al concentrations in the reaction layers and remaining filler metal appear to be counter-intuitive vis-a-vis the brazing conditions. That is, the more severe brazing conditions caused *less* Al in the reaction layers and *negligible* Al in the filler metal while the less severe brazing conditions caused higher Al concentrations in both the reaction layers and filler metal. This apparent discrepancy can be explained by the 995°C (1769°F), 20 min brazing conditions caused thicker reaction layers (5.5±0.6 μm); a greater degree of recrystallization in the KovarTM base material; and more extensive run-out. However, given how quickly the Al/ KovarTM base material reaction occurs, it is unlikely that the reduced Al concentration in the reaction layer was caused by these factors. Rather, the reaction layer compositions was determined by the chemical potential as established by the filler metal composition and brazing parameters.

The Fe, Ni, Co, and Al concentrations were measured in the Ag-5Al filler metal. Those values were (wt.-%): Fe, 0.79±0.10; Ni, 0.48±0.06; Co, 0.36±0.05; Al, 0.07±0.01. The more severe brazing conditions caused the concentrations of Fe, Ni, and Co to more than double those measured after brazing at 965°C (1769°F) for 5 min. Nevertheless, these concentrations remained below the solubility limit upon solidification. The SEM images confirmed an absence of precipitate phases in the filler metal.

The optical images in Fig. 2d showed extensive run-out by the Ag-10Al filler metal under all brazing conditions. Run-out behavior is shown by the SEM photographs in Fig. 14. The brazing conditions were 965°C (1769°F) and 5 min. The inset image in Fig. 14a documents the extent of filler metal travel, which extended from the gap along the flange edges to the latters' corners (orange arrows). The high magnification image shows the development of thick reaction layers under the filler metal. A second location is shown in Fig. 14b where the filler metal wet and spread only to the edge of the gap (orange arrows). The reaction layer extended a short distance beyond the filler metal. These images establish that the reaction layer is a necessary, but not sufficient, condition for run-out by the filler metal. Capillary flow is also a necessary condition. However, the Ag-0Al filler metal showed that, in the absence of the reaction layer, capillary flow is not a sufficient condition for run-out.

Figure 15a is an SEM image shows Ag-10Al braze joint microstructure. Cracks were prevalent in the reaction layers as was recrystallization in the neighboring KovarTM base material. Crack development is also apparent in the reaction layers. The reaction layer thickness was $5.7\pm0.5~\mu m$ and, like the reaction layer microstructure, showed no significant correlation to gap clearance ($R^2=0.46$).

The SEM image in Fig. 15b shows a high magnification view of the reaction layer (yellow box, Fig. 15a). The cracks initiated in the dark phase at the reaction layer's interface with the Ag-10 filler metal. Some cracks propagated along pre-existing grain boundaries in the reaction layer (blue arrow). The absence of filler metal in the cracks indicates that they developed *after* solidification of joint. The recrystallization zone is visible in the Kovar™ base material as well as is the Fe-rich reaction layer between the latter and the reaction layer.

Figure 16 is a cross section, SEM photograph of one of two isolated locations where the particle phase developed within the Ag-10Al filler metal. A similar microstructure was observed in Ag-10Al, sessile drop test samples fabricated under the same brazing conditions [3]. The

braze joint gap did not exhibit any distinguishing features – e.g., gap clearance extremes, abnormal interface structure, etc. – that would predict particle formation at those particular locations. This SEM image confirmed that the particles were formed by the same spalling mechanism proposed in reference 3 (magenta arrows).

A representative EPMA trace 1 is shown in Fig. 17a. All traces were taken at locations without particles. The cyan arrows point to the reaction layers. The red arrows identify the Ferich reaction layers, which was more limited on the left-hand side reaction layer versus right-hand side location. The remaining filler metal contained 4.6±0.2 wt.% Al, which implies that there was more than enough Al to support reaction layer formation, including under the run-out layers. The remaining filler metal contained Fe, Ni, and Co at the following concentrations: 0.16±0.08; Ni, 0.09±0.05, and Co, 0.10±0.04 wt.%, respectively. These values, individually and summed together (0.4±0.2 wt.%), were less than similar metrics for the previous Ag-xAl filler cases. This observation was unexpected, given the high Al content in the filler metal and that the driving force for Al to react with Fe, Ni, and Co would accelerate the dissolution process.

Figure 17b provided an enlarged view of the left-hand interface. This location did not exhibit significant recrystallization in the Kovar[™] base material. The Ni and Co signals exhibited large and small minima, respectively, that coincided with Fe-rich reaction layer (red arrow). The Fe and Ni concentrations exhibited large fluctuations within reaction layer that were out-of-step with each another. The Co signal exhibited a concentration profile similar to the Ni signal but having a lesser amplitude.

Referring to the immediate interface between the reaction layer and filler metal field, the Fe, Ni, and Co signals exhibited a small gradient extending approximately $1-2~\mu m$ into the filler metal. This distance is at the resolution limit of the EPMA technique.

The three black arrows identify the locations at which were calculated the following low-Al, medium-Al, and high-Al phases:

- Low-Al composition: (Fe, Ni, Co)_{79±8}Al_{21±2} \approx (Fe, Ni, Co)₄Al
- Medium-Al composition: (Fe, Ni, Co)_{68±6}Al_{32±3} \approx (Fe, Ni, Co)₂Al
- High-Al composition: (Fe, Ni, Co)_{55±6}Al_{45±1} \approx (Fe, Ni, Co)₆Al₅

The above compositions were compared to those that characterized the Ag-5Al filler metal when it was brazed with the same parameters of 965°C (1769°F) and 5 min. The low- and medium-Al phases had the same compositions to within experimental error. The high-Al phases differed slightly in Al concentrations: 45±1 at.% for the current Ag-10Al alloy versus 41±2 at.% for the previous Ag-5Al alloy. Yet, despite these small composition differences, the reaction layer was susceptible to cracking in the Ag-10Al filler metal but not so in the Ag-5Al filler metal.

There are two scenarios, acting either separately or in combination, that explain the cracks: (a) the slightly higher Al concentration in the high-Al phase formed by the Ag-10Al alloy or (b) the higher Al concentration remaining in the Ag-10Al filler metal increased the residual stresses in the reaction layer. The latter scenario assumes that the higher Al content in the filler metal increased it strength, causing it was less compliant towards relieving CTE mismatch, residual stresses. These scenarios are explored further, later on.

The braze joints were examined that were brazed at 965°C (1769°F) for 20 min. Figure 2d showed extensive run-out of the filler metal. The braze joint microstructures were very similar to those observed after 5 min (Figs. 14 – 16). Cracks initiated in the high-Al phase next to the filler metal and stopped in the low-Al phase prior to reaching the KovarTM base material. The reaction layer thickness was 6.8±0.7 μm and did not show a significant dependence on gap clearance. This value was higher than that measured after 5 min, 5.7±0.5 μm, and exceeded the thicknesses of 3.2±0.8 μm and 4.7±0.8 μm that formed with the Ag-2Al and Ag-5Al filler metals, respectively, under the same brazing conditions. A few gap locations had particle phase

present in the filler metal. Again, the appearance of the particles did not depend upon gap clearance or another microstructural feature.

The Ag-10Al braze joints, which were fabricated at 995°C (1823°F) and 5 min, showed extensive run-out per Figure 2d. The same crack morphology was observed in the reaction layers as described above. The reaction layer thickness remained constant with a value of $6.5\pm0.5~\mu m$.

Braze joints were examined that were fabricated with the Ag-10Al filler metal and using the most severe conditions of 995°C (1823°F) and 20 min. The backscattered electron (BSE) channeling image is shown in Fig. 18a that accentuates the extensive recrystallization zones in the adjoining KovarTM base material. Figure 18a also shows the extensive grain structure in the reaction layers. This gap clearance was very small, averaging a little over 5 μm. Although some locations exhibited gap clearances a large as 53 μm, the reaction layer had a consistent thickness, which was measured to be 7.7±0.5 μm.

Figure 18a showed the grain boundaries to have generally a vertical or columnar orientation. However, horizontal grain boundaries were also observed in the layers. Figure 18b is a high magnification image of the reaction layer location identified by the yellow box in Fig. 18a. The green arrow points to one such horizontal boundary. The presence of horizontal boundaries implies that further grain development occurred after initial formation of the reaction layer.

The SEM image in Fig. 18b shows the Fe-rich phase along the reaction layer / Kovar™ base material interface. Recrystallization was extensive in base material. Three gray tones — light, dark, and "very dark" — suggested that three phase composition comprised the reaction layer.

The two SEM images in Fig. 19 show cracks that propagated in the reaction layers as well through the Ag-10Al filler metal. Figure 19a has a crack that crossed the Ag-10Al filler

while that in Fig. 19b showed cracks in the filler metal and particles. The presence of cracks in the filler metal implies that it has a higher strength and concurrently, lower ductility. These observations lend further evidence of scenario (b) described above, that the increased susceptibility to reaction layer cracking is caused by a reduced ability of the filler metal to relieve CTE mismatch residual stresses.

The Ag-10Al braze joint [995°C (1823°F), 20 min] was examined at a terminus of its capillary flow. See Fig. 20. The inset image shows filler metal flow through the gap. The high magnification photograph (yellow box in the inset photograph) shows reaction layers had formed beyond the filler metal on both sides of the empty gap. Cracks were absent in the reaction layer on both sides of the unfilled gap, but present in the reaction layer adjacent to the filler metal. This observation implies that the cracks are not an intrinsic property of the reaction layer. Rather, the Ag-10Al filler metal is a necessary factor, *mechanically*, in their formation.

The EPMA data are exemplified by trace 2 in Fig. 21a, which shows the elemental concentrations across the entire braze joint. Of particular note was the elevated Al concentration remaining in the filler metal, 7.8±0.1 wt.%. This value represented a significant proportion of the 10 wt.% Al originally present in the filler metal. The remaining Al concentration was well in excess of the 4.6±0.2 wt.% present in the Ag-10Al filler metal after brazing at 965°C (1769°F) for 5 min. The expectation was that the higher brazing temperature and longer time would promote a greater extent of reaction between Al and the Kovar™ base material, thus leaving the filler metal with an Al concentration that was less than the 4.6 wt.%. This unexpected behavior implies that brazing temperature and time effects are determined by driving force (chemical potential) of the reaction as opposed to simply accelerating the latter's thermally-activated, rate kinetics.

The concentrations were compiled of Fe, Ni, and Co in the filler metal. Those values, which were: Fe, 0.10±0.05; Ni, 0.06±0.03; Co, 0.07±0.03 wt.%, were below their respective

solubility limits in Ag so that second phases were not formed by them. More importantly, these concentrations were similar to those measured in the filler metal after brazing at 965°C (1769°F) and 5 min, despite the harsher process parameters. This behavior implies that the dependence of base material dissolution on the brazing process parameters, like the reaction layer formation, was not based solely on thermal activation effects.

The details of the interface microstructure are shown in Fig. 21b, which is the EMPA trace of the left-hand side of the joint belonging to trace 2. The red arrow indicates the Fe-rich phase adjacent to the Kovar™ base material. Recrystallization (dashed blue arrow) was extensive in the base material; albeit, it was more limited at this particular location. As observed in previous analyses, the Fe peak (red arrow) is accompanied by a minimum in the Ni concentration and a drop off by the Co signal. The Al concentration increased largely monotonically towards the filler metal interface. Iron and Ni exhibited fluctuations in the reaction layer: a minimum in the Fe signal and maximum Ni signal, respectively. The Co remained relatively constant before dropping towards zero near the reaction layer/filler metal interface. The "very dark" phase in Fig. 18b corresponds to a peak of Al signal at the same interface. Progressing from the interface into the filler metal, Fe, Ni, and Co exhibited small concentration gradients that were barely greater than the sampling volume of the EPMA technique.

The reaction layer compositions were determined at the three black arrows shown in Fig. 21b and are shown, below:

- Low-Al composition: (Fe, Ni, Co)_{75±6}Al_{25±2} \approx (Fe, Ni, Co)₃Al
- Medium-Al composition: (Fe, Ni, Co)_{68±4}Al_{32±2} \approx (Fe, Ni, Co)₂Al
- High-Al composition: (Fe, Ni, Co)_{59±10}Al_{41,3±0.9} \approx (Fe, Ni, Co)₃Al₂

These compositions were compared to those observed for the same Ag-10Al filler metal, but brazed at 965°C (1769°F) for 5 min. The low-Al phase exhibited a small increase of Al content from 21±2 at.% to 25±2 at.%. A significant change was not observed in the medium-Al composition. The high-Al phase exhibited an Al content of 41±1 at.%, which was less than the 45±1 at.% observed after brazing at 965°C (1769°F) and 5 min. By-and-large, the harsher process conditions altered only slightly the composition makeup of the reaction layer. Moreover, an ample reserve of Al was present in the filler metal. These observations further substantiate the point that system chemical potential controlled the reaction layer composition as opposed to faster rate kinetics.

Discussion

A considerable amount of reaction layer data – thicknesses, microstructure, and composition measurements – have been presented in this report. In addition, there are important findings reported in Part 1, which were obtained from the sessile drop configuration. The objective of this section is to pull together all results to determine the root-cause for the runout phenomenon. The analyses are organized into four topical areas: visual observations as well as reaction layer composition, microstructure, and thickness data.

Visual observations

Capillary forces have a significant role in run-out by the molten filler metal. First, the sessile drop samples in Part 1did not exhibit run-out lobes. Those specimens did exhibit a sharp increase of *general* wetting and spreading between 2 wt.% Al and 5wt% Al filler metal additions, which was correlated to an increased Al concentration in the reaction layer. Secondly, as a sessile drop, the Ag-0Al filler metal did not exhibit wetting and spreading on the Kovar™ surface. However, when placed between two Kovar™ base materials, capillary forces

caused the filler metal to flow in the gap without the presence of a reaction layer (Fig. 4). Third, capillary flow is required to form the run-out lobes in the alumina/Kovar™ base material joints (Fig. 1). The redox reaction that takes place at the filler metal/alumina interface was shown in the reference 1 study to be unable to support run-out by itself.

Typically, only one or, at most, two lobes are observed with run-out (Fig. 1). The analysis in Part 1 suggested that the lobe geometry resulted from a *localized* acceleration of wetting and spreading by the filler metal [3]. The scenario was presented whereby the *localized* Al concentration exceeded 2-5 wt.% in the filler metal, leading to the local formation of the high-Al, reaction layer (Al > 30 at.%) and thus, the run-out lob. However, the present braze joint data did not show evidence of a spatial variation of Al concentration across the reaction layer of each Ag-xAl filler metal. Moreover, the images in Fig. 2 show run-out took place on a broader spatial scale than is reflected by typical active braze joints (e.g., Fig. 1).

The above analysis indicates that the lobe configuration does not result from a localized increase of Al in the filler metal and subsequent, localized, high-Al reaction layer. Rather, the limited number of run-out lobes is a consequence of the surface tension of the molten filler metal. The increase of the atmosphere/filler metal interfacial area, which results from the initial one or two run-out lobes, reduces the driving force (chemical potential) sufficiently to mitigate the formation of any other run-out events (lobes), even in the presence of capillary flow. Those first lobes are simply a stochastic event – that is, the joint microstructure does not have a feature that causes a run-out lobe to occur at one location or another site.

In conclusion, visual observations indicated that there is a strong propensity for run-out to occur in the braze joint configuration when the overall Al concentration in the filler metal was greater than, or equal to, 2 wt.%. The Ag-0Al filler metal exhibited capillary flow, but not run-out. Therefore, capillary flow is a necessary, *but not sufficient*, condition for run-out lobes. The reaction layer is also a necessary contributor; but, it is not sufficient since run-out lobes were not

observed in the sessile drop configuration (Part 1). Lastly, the limit of run-out lobes to one, or at most two, is a surface tension effect.

Reaction layer compositions

The relationship between reaction layer composition and run-out was further investigated by graphing the Al concentration (at.%) of the reaction layer phase that directly contacted the molten filler metal as a function of Al concentration in the filler metal (wt.%). The graph appears in Fig. 22. The filled symbols, together with the solid blue and red lines, represent the braze joint data for the present brazing conditions of 965°C (1769°F), 5 min and 995°C (1823°F), 20 min, respectively. The general trend has Al concentration in the reaction layer phase increase with increasing Al content in the filler metal. The less-severe brazing conditions led to higher Al concentrations in the reaction layer for the Ag-5Al and Ag-10Al filler metals. The same behavior was observed for the *average* reaction layer concentrations of the Ag-2Al filler metal; but, the difference was not statistically significant. This somewhat counter-intuitive trend is further evidence that the brazing time and temperature affect the phase compositions through the chemical potential rather than thermally-activated, rate kinetics.

A comparison was made between these results and similar findings for the sessile drop configuration. The plot in Fig. 22 also includes the same phase concentration data that was compiled from the Part 1 sessile drop study. Those results, which are represented by the open symbols and dashed lines, showed the same trend of a greater Al concentration in the high-Al phase for the less severe brazing conditions. In addition, the high-Al phase had considerably higher Al concentrations in the sessile drop geometry than it did in the joint geometry, even when run-out was very limited for the Ag-2Al filler metal. This comparison shows the reaction layer phase has a relatively large Al concentration range that is sensitive to the sessile drop versus braze joint geometry.

As noted previously, a sharp increase was observed for wetting and spreading by the Ag-xAl sessile drops between 2 wt.% and 5 wt.%. Referring to Fig. 22, the corresponding, high-Al reaction layer phase had an Al content that exceeded 30 at.%. In the case of the braze joint, runout occurred when the Al concentration was greater than, or equal to, 25 at.% (Ag-2Al filler metal). This comparison shows that capillary flow provided the additional driving force for runout to occur at the lower Al concentration in the reaction layer.

Figure 23 shows Al concentrations in the medium-Al and low-Al reaction layer phases. The medium-Al phase exhibited the same trend as that of the high-Al phase; that is, the Al concentration increased with Al content in the Ag-xAl filler metal. However, the Al concentration was statistically greater for the 965°C (1769°F), 5 min process condition only in the case of Ag-5Al. The low-Al phase had an Al concentration in the range of 20 – 25 at.%, regardless of filler metal composition or process parameters. The same trend was observed for the sessile drop samples except for a tighter, Al concentration range of 24 – 26 at.%. Therefore, the sensitivity of reaction layer composition to sessile drop versus joint configuration is reflected only in the high-Al phase; the low-Al phase had a similar composition for both geometries.

In summary, run-out occurred in the joint configuration when the Al concentration in the filler metal was greater than, or equal to, 2 wt.%. That concentration gave rise to an Al content of greater than, or equal to, 25 at.% in the reaction layer directly contacting the (molten) filler metal. The latter concentration was lower than the "greater than 30 at.% Al" benchmark for the accelerated wetting and spreading behavior by the sessile drops (Ag-xAl, 2 < x < 5 wt.%). Therefore, capillary flow allowed for run-out to take place at a lower Al concentration in filler metal and in the reaction layer. Figure 23 showed that the medium-Al composition (joint geometry) was also controlled by the filler metal composition and to a lesser degree, by the brazing process parameters. The Al concentration in the low-Al phase remained statistically

unchanged as a function of filler metal composition and brazing parameters and was similar to that measured for the sessile drop samples.

Braze joint microstructure

The SEM images documented the changes that took place to the reaction layer microstructures as a function of brazing parameters and filler metal composition. Of particular interest was the occurrence of cracks. Figure 22 shows the Al concentration in the corresponding reaction layer. A reaction layer was *absent* at the Kovar™/Ag-0Al interface to within the resolution limit of the EPMA. Cracks were not observed in the reaction layers of any of the Ag-2Al samples regardless of brazing parameters. Similarly, the reaction layers belonging to the Ag-5Al filler metal did not exhibit cracks, despite significant higher Al concentrations. Lastly, the Ag-10Al filler metal generated the high-Al, reaction layer phase having Al contents that exceeded 40 at.%. *Cracks were present in the reaction layers for all brazing process conditions*.

The root-cause analysis of the cracks begins by considering that, when brazed at 995°C (1823°F) and 20 min, the Ag-10Al filler metal formed a high-Al reaction layer phase with an Al concentration of 41 at.%. Cracks were present. Under the same brazing conditions, the Ag-5Al filler metal generated a high-Al phase having only 30 at.% Al. Cracks were absent. This comparison suggests a correlation between increased Al content of the high-Al phase and cracks in the reaction layers. (Recall that cracks initiate in the high-Al phase.) However, when the same comparison was then made between the Ag-5A and Ag-10Al filler metals after brazing at 965°C (1769°F) for 5 min, the corresponding, high-Al phases had similar Al concentrations of 41.3±0.7 at.% and 45±1 at.% for the, respectively. Yet, cracks were absent in the former case and present in the latter case. The difference of Al contents seemed hardly sufficient to "turn on/turn off" the cracking mechanism. Therefore, the Al content of the reaction layer was not the

only factor contributing to cracks. Recall that cracks did not appear to be an intrinsic feature of reaction layers created by the Ag-10Al filler metal – see Fig. 20.

The search for a second factor turned to the *post-braze*, filler metal composition. Figure 24 shows a plot of the Al concentration in the filler metal as a function of the nominal (or starting) Al content of the filler metal. The brazing conditions were 965°C (1769°F), 5 min and 995°C (1823°F), 20 min. The error bars are only slightly larger than the symbols. The Al concentration increased above trace levels with the Ag-5Al filler metal after brazing at 965°C (1769°F) for 5 min, where it reached 1.8 \pm 0.1 wt.%. The Al concentration increased further to 4.6 \pm 0.2 wt.% for the Ag-10Al alloy. Cracks appeared in the reaction layer. The more severe brazing conditions of 995°C (1823°F) and 20 min caused negligible Al to remain in the Ag-2Al and Ag-5Al filler metals. The Al concentration increased significantly to 7.8 \pm 0.1 wt.% for the Ag-10Al filler metal. Reaction layer cracks appeared in the latter case.

The second contribution affecting crack development was that Al additions increase the strength of Ag-xAl-alloys. A study by G. Sachs showed that Ag-Al alloys exhibit a more than a 50% increase in hardness and 20% decrease of elongation with Al additions up to 5 wt.% [6]. As described by Jordan, et al., Seftel and Sachs reported a rapid loss of ductility when the Al content exceeded 5 wt.% [7]. The authors concluded that Al additions exceeding the 5.3 wt.% solid-solution limit, formed intermetallic compound phases upon solidification that precipitation hardened the alloy. Microstructural evidence was not provided in either reference. Also, precipitated particles were not observed in the present study using the SEM technique, albeit, the Al concentrations approached $(4.6 \pm 0.2 \text{ wt.%})$, or exceeded $(7.8 \pm 0.1 \text{ wt.%})$, the solubility limit in Ag. This analysis implies that reaction layer cracks resulted from a loss of ductility by the Ag-xAl filler metal, rendering the latter less effective at reducing the residual stresses caused by the thermal expansion mismatch between it and the Kovar TM base material.

The role of Fe, Ni, and Co traces to the filler metal was also considered vis-à-vis the crack behavior. The three elemental concentrations were combined as a single pseudo-constituent. Figure 25 shows a plot of the combined concentrations as a function of nominal Al concentration in the filler metal. The error bars are the sum of the standard deviations from each of the three elements. Although the mean values showed a slightly decreasing trend versus filler metal concentration for the 965°C (1769°F), 5 min process, they were unchanged, statistically. On the other hand, a maximum occurred at Ag-5Al when the brazing process was 995°C (1823°F) and 20 min. The reaction layers did not exhibit cracks for this filler metal. The lowest concentration of Fe+Ni+Co occurred with the Ag-10Al alloy where cracking was prominent. Therefore, a correlation cannot be developed between the total concentration of Fe, Ni, and Co versus crack development. Lastly, Fig. 25 clearly shows that the Fe+Ni+Co concentrations resulted from a complex interaction between the Kovar™ base material, the filler metal composition (Al content); and the process conditions. The Fe, Ni, and Co concentrations were not simply a function of dissolution as determined by thermally-activated rate kinetics.

Particles were observed at a few isolated locations in the gaps of the Ag-10Al filler metal (Figs. 16 and 19b). The phase composition replicated that of the reaction layers as determined in Part 1 and their source was spalling of the reaction layer into the filler metal. Their origin was an accelerated growth by the reaction layer. The mechanism is likely the same stochastic behavior as that responsible for initiating run-out lobes. A loss of driving force cause localization of the particle; however, the surface tension effect is an unlikely candidate for this process.

In summary, reaction layer cracking, which was observed only with the Ag-10Al filler metal, was attributed to the latter's strengthening by higher residual Al concentrations. The elevated strength impeded the relaxation of residual stresses caused by thermal expansion mismatch between the filler metal and Kovar™ base material. Trace concentrations of Fe, Ni, and Co in the filler metal did not have a first-order effect as was also the case for the limited

development of the large particles. The isolated spalling of particles from the reaction layer results from an instability in the reaction layer rate kinetics. The source has not been identified for this behavior.

Reaction layer thickness

The reaction layer thicknesses were plotted in Fig. 26 as a function the nominal Al content of the filler metal. Separate traces were provided for each of the four brazing process conditions. The error bars represent ±one standard deviation and were included only with the 965°C (1769°F), 5 min and 995°C (1823°F), 20 min data. The error bars were similar for the other brazing conditions but omitted for clarity. Generally, reaction layer thickness increased with Al concentration in the Ag-xAl filler metal. However, statistically-significant trends could not be discerned between the individual process conditions with the exception of the Ag-10Al alloy and the two extreme process condition. Rather, layer thickness was controlled largely by the *nominal* Al content of the filler metal.

In summary, the reaction layer thickness increased with Al concentration in the Ag-xAl filler metal. The thickness did not exhibit a statistically-significant difference as a function of brazing process parameters with the exception of a single case. This trend implies that the layer thicknesses, like their associated compositions, were not solely dependent upon thermally-activated, rate kinetics (brazing parameters) but rather, were controlled by the chemical potential (driving force) determined primarily by the filler metal composition.

Conclusions

1. A study was performed, which examined the microstructural characteristics of braze joints made between two KovarTM base materials using the filler metals, Ag-xAl, having x = 0, 2, 5,

- and 10 wt.% Al. The brazing temperatures were 965°C (1769°F) and 995°C and brazing times, 5 and 20 min. The entire process was performed under high vacuum.
- 2. Run-out occurred in the presence of capillary flow (joint geometry) and the Al concentration in the filler metal was greater than, or equal to, 2 wt.%. The latter condition corresponded to an Al content, y, in the interface reaction layer, (Fe, Ni, Co)_xAl_y that was greater than, or equal to, 25 at.%.
- 3. Reaction layer cracking, which was observed only with the Ag-10Al filler metal for all brazing conditions, was attributed to strengthening of the filler metal by high residual Al concentrations that prevented the relaxation of thermal expansion mismatch stresses. Trace concentrations of Fe, Ni, and Co did not have a first-order effect.
- 4. Isolated patches of the particles were observed in the Ag-10Al filler metal, which spalled from the reaction layer growth, were the result of a locally accelerated growth.
- 5. The reaction layer thickness increased with Al concentration in the Ag-xAl filler metal, but generally did not exhibit a consistent dependency on brazing process parameters. This trend indicated that layer growth was not dependent solely upon thermally-activated, rate kinetics but rather, the chemical potential (driving force) determined by the composition of the Ag-xAl filler metal.
- 6. Applications will rely upon braze *joints*, which because of the presence capillary flow, can potentially exhibit run-out. Present data suggests that run-out mitigation would require the Al content of the filler metal remain less than 2 wt.% in the presence of the Kovar™ base material.

Acknowledgements

The authors wish to thank Ms. Rebecca Wheeling for a thorough review of the manuscript. Sandia National Laboratories is a multi-mission laboratory managed and operated by National Technology and Engineering Solutions of Sandia LLC, a wholly owned subsidiary of Honeywell

International Inc. for the U.S. Department of Energy's National Nuclear Security Administration under contract DE-NA0003525.

References

[1] Vianco, P. T., Walker, C. A., De Smet, D., Kilgo, A. C., Mckenzie, B. M., Kotula, P. M., and Grant, R. L., 2015. Understanding the run-out behavior of a Ag-Cu-Zr braze alloy when used to join alumina to an Fe-Ni-Co alloy. *Proc.* 6th *International Brazing and Soldering Conference*. eds. R. Gourley and C. Walker, CD-ROM. American Welding Society.

[2] KovarTM is a registered trademark of Carpenter Technologies, Reading, PA.

[3] Vianco, P. T., Walker, C. A., De Smet, D., Kilgo, A. C., Mckenzie, B. M., and Grant, R. L., 2018. Interface reactions responsible for run-out in active brazing: Part 1. *Welding Journal Res. Suppl.* 97(2) pp. 35s-54s.

[4] Binary Alloy Phase Diagrams: Volume 1. Ed. by T. Massalski (ASM, Inter., Materials Park, OH; 1986) pp. 16, 25, and 48.

[5] Massalski, T. ibid, pg. 3.

[6] Sachs, G., *Pracktische Metallkunde*," Chapt. 7, "Verfetigung von Legierungen (Springer, Berlin, Germany; 1934) DOI: 10.1007/978-3-7091-5320-8.

[7] Jordan, L, Grenell, L, and Herschman, H., 1927. Tarnish resisting silver alloys. *Technology Papers of the Bureau of Standards, No. 348*. (US. Govt. Printing Office, Washington, DC; 1927) pp. 472 – 473.

Figures

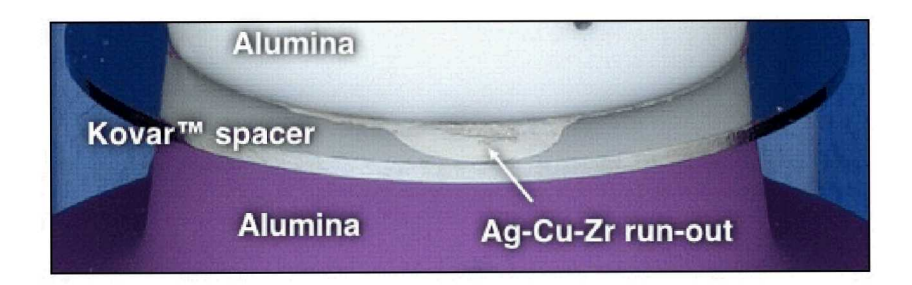
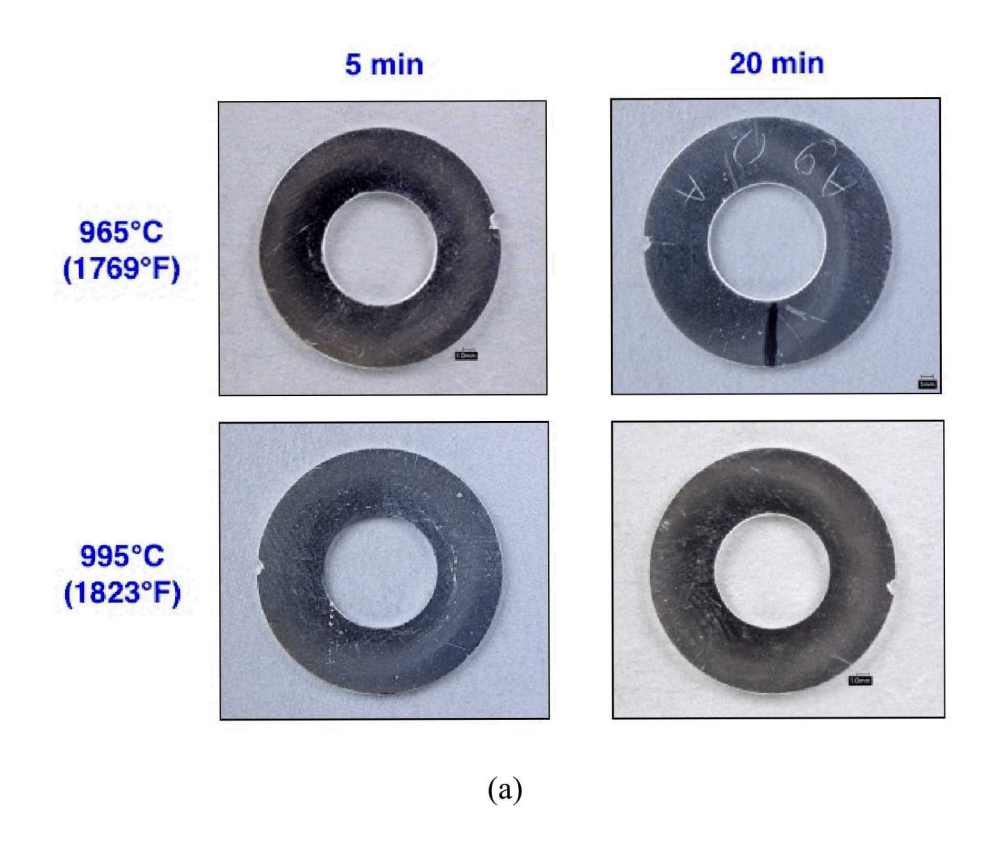


Figure 1 Photograph shows run-out by the Ag-Cu-Zr active braze alloy used to join alumina base materials ("buttons") to the Kovar $^{\text{TM}}$ spacer.



5 min 20 min 965°C (1769°F) 995°C (1823°F) (b) 5 min 20 min 965°C (1769°F) 995°C (1823°F) (c)

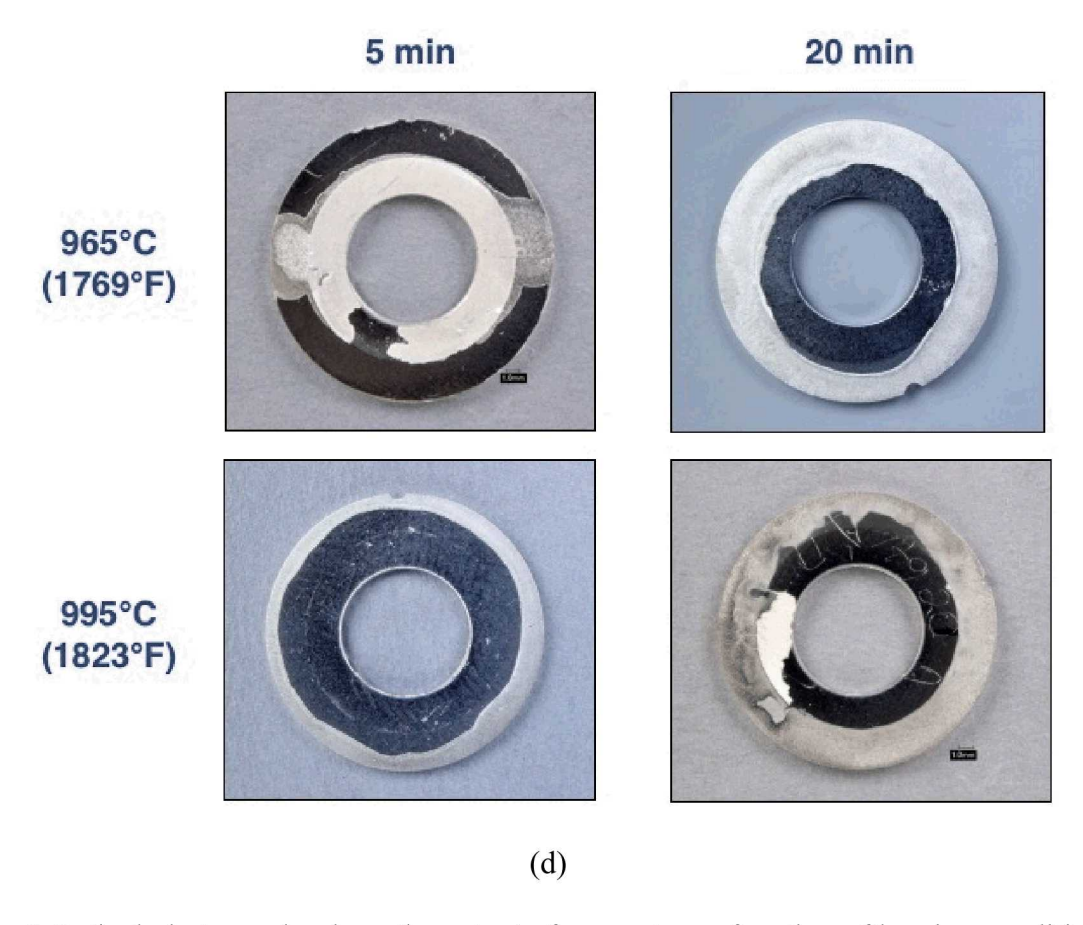


Figure 2 Optical photographs show the extent of run-out as a function of brazing conditions and filler metal composition: (a) 0 wt.% Al, (b) 2 wt.% Al, (c) 5 wt.% Al and (d) 10 wt.% Al.

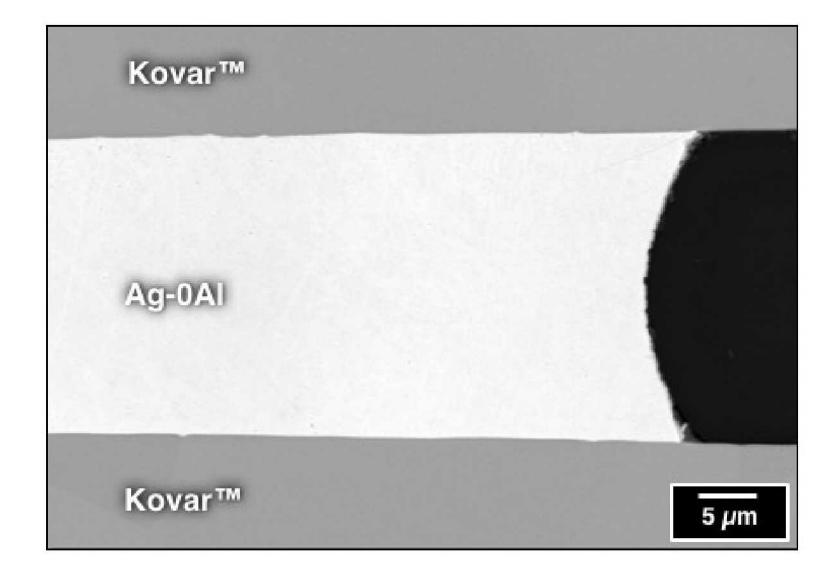


Figure 3 SEM photograph shows the cross section of the Ag-0Al test specimen fabricated at 965°C (1769°F) and 5 min.

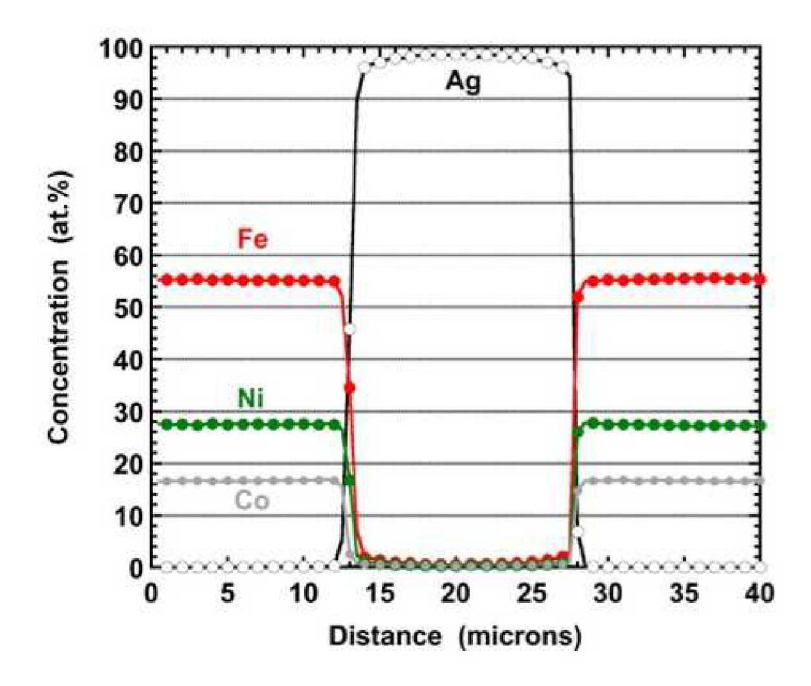


Figure 4 Plot shows the EPMA trace made across the gap of the braze joint made with the Ag-0Al filler metal. The brazing conditions were 995°C (1823°F) and 5 min.

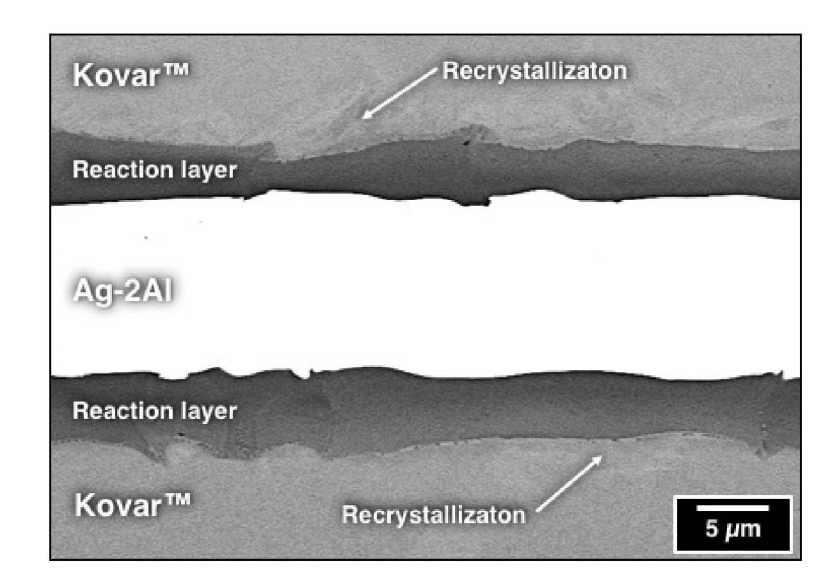


Figure 5 SEM photograph shows the braze joint of the sample fabricated with the Ag-2Al filler metal under the conditions of 965°C (1769°F) and 5 min. The image illustrates the reaction layer for a 5 μ m joint clearance.

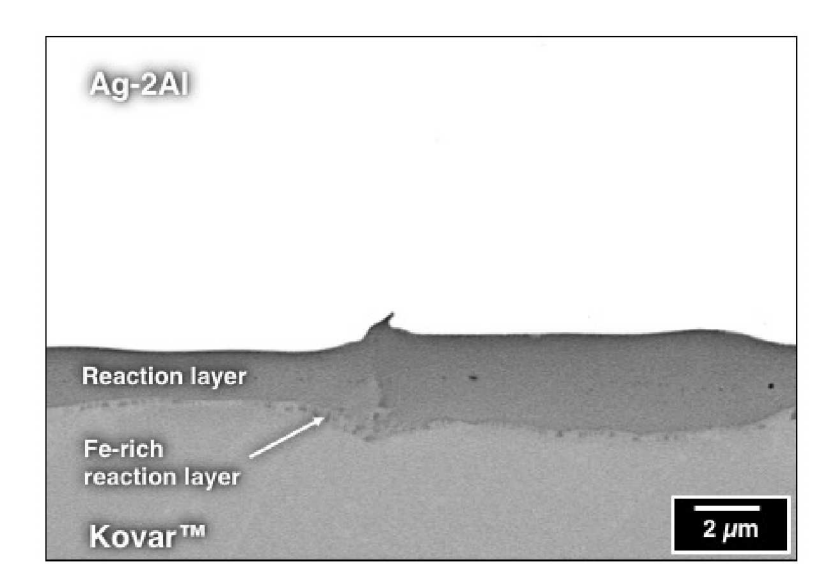
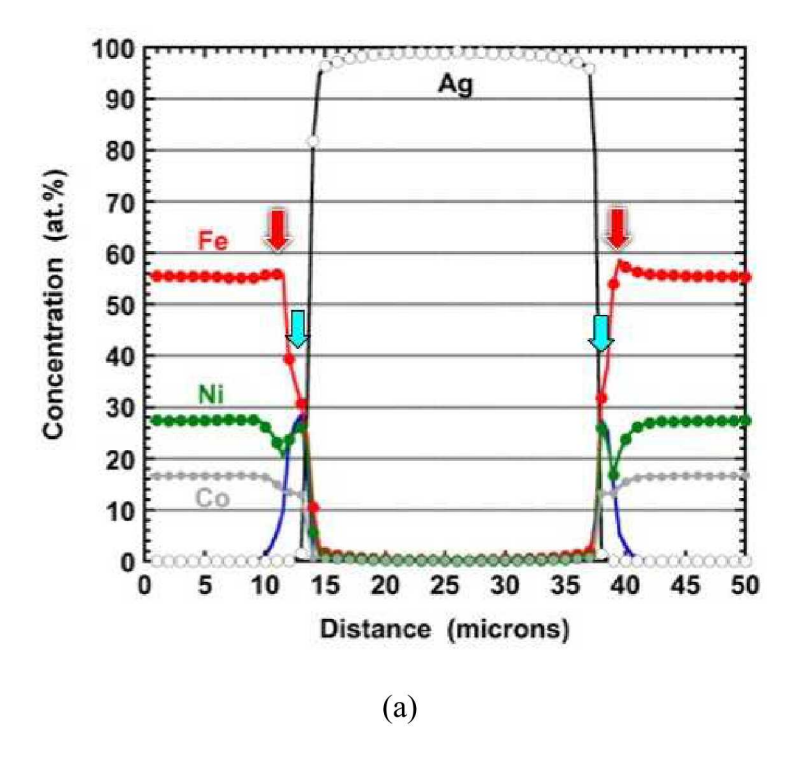


Figure 6 SEM photograph shows the interface and reaction layer microstructures belonging to the Ag-2Al filler metal brazed at 965°C (1769°F) for 5 min.



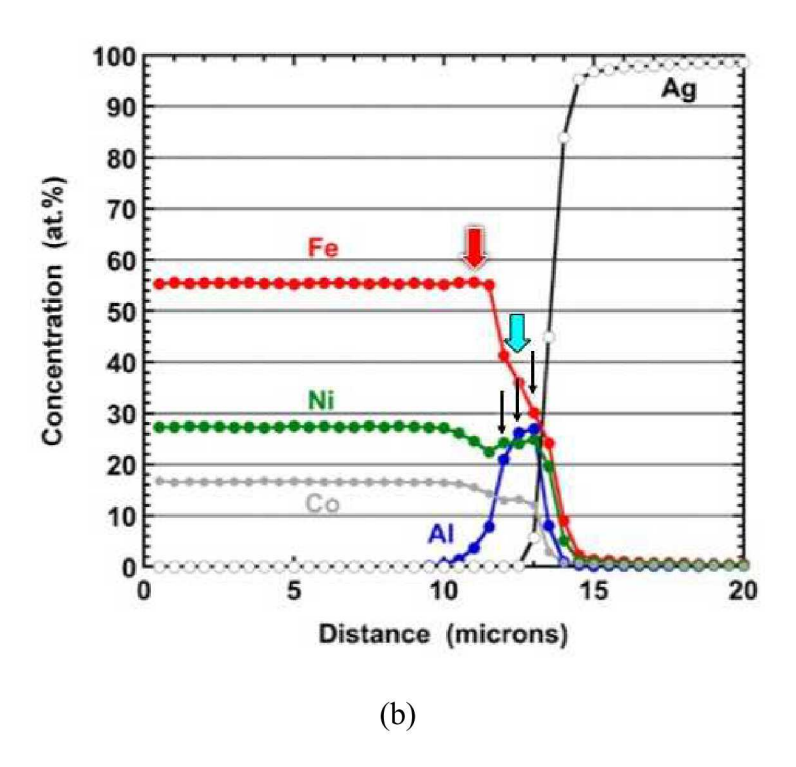


Figure 7 (a) EPMA trace across the braze joint formed by the Ag-2Al filler metal under the brazing conditions of 965°C (1769°F) and 5 min. The cyan arrows indicate the location of the reaction layers. (b) Enlarged segment of the EPMA trace shows the left-hand side reaction layer, KovarTM base material, and Ag-2Al filler metal. The red arrows indicate the Fe-rich reaction layer adjacent to the base material. The black arrows indicate the measurement points of the low-Al, medium-Al, and high-Al concentrations (left-to-right).

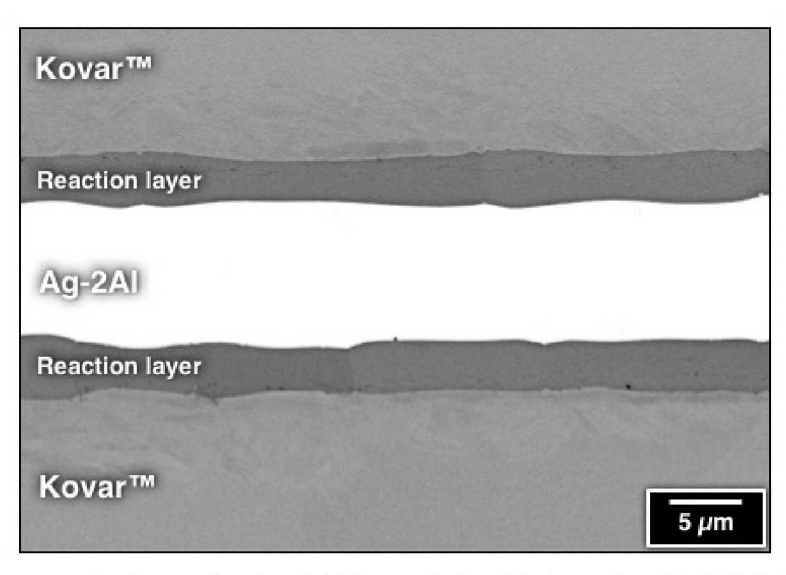


Figure 8 SEM photograph shows the Ag-2Al braze joint fabricated at 995°C (1823°F) and 20 min.

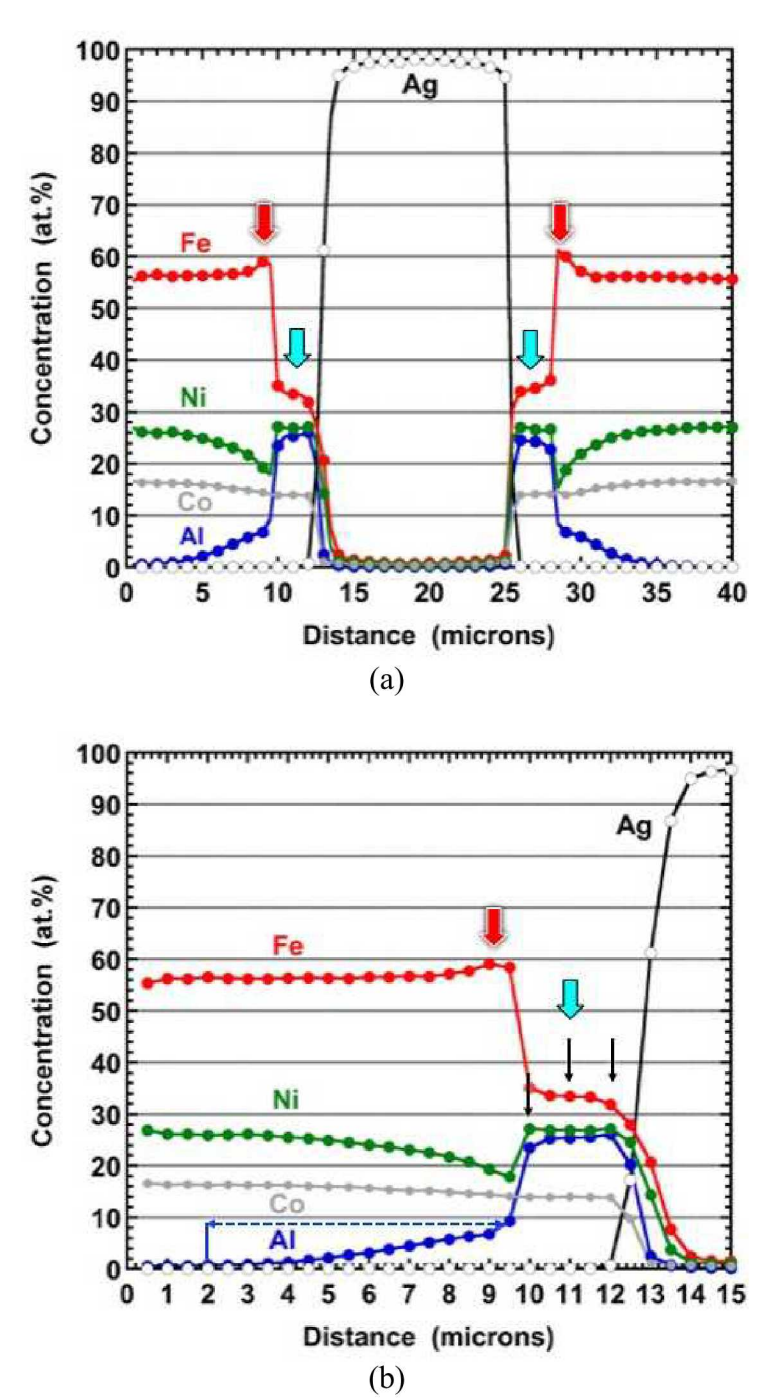


Figure 9 (a) EPMA data obtained from the braze joint fabricated with the Ag-2Al filler metal and brazing conditions of 995°C (1823°F) and 20 min. The red and cyan arrows are the Fe-rich reaction layer and Al-based reaction layers, respectively. (b) Enlarged EPMA trace focuses on the left-hand reaction. The blue arrow identifies a recrystallization zone. The black arrows indicate the measurement points of the low-Al, medium-Al, and high-Al concentrations (left-to-right).

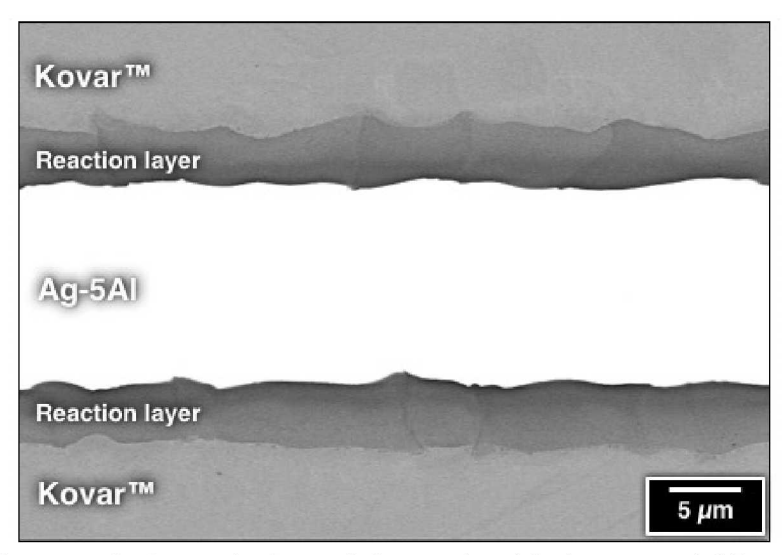


Figure 10 SEM photograph shows the braze joint made with the Ag-5Al filler metal. The brazing conditions were 965°C (1769°F) and 5 min time duration.

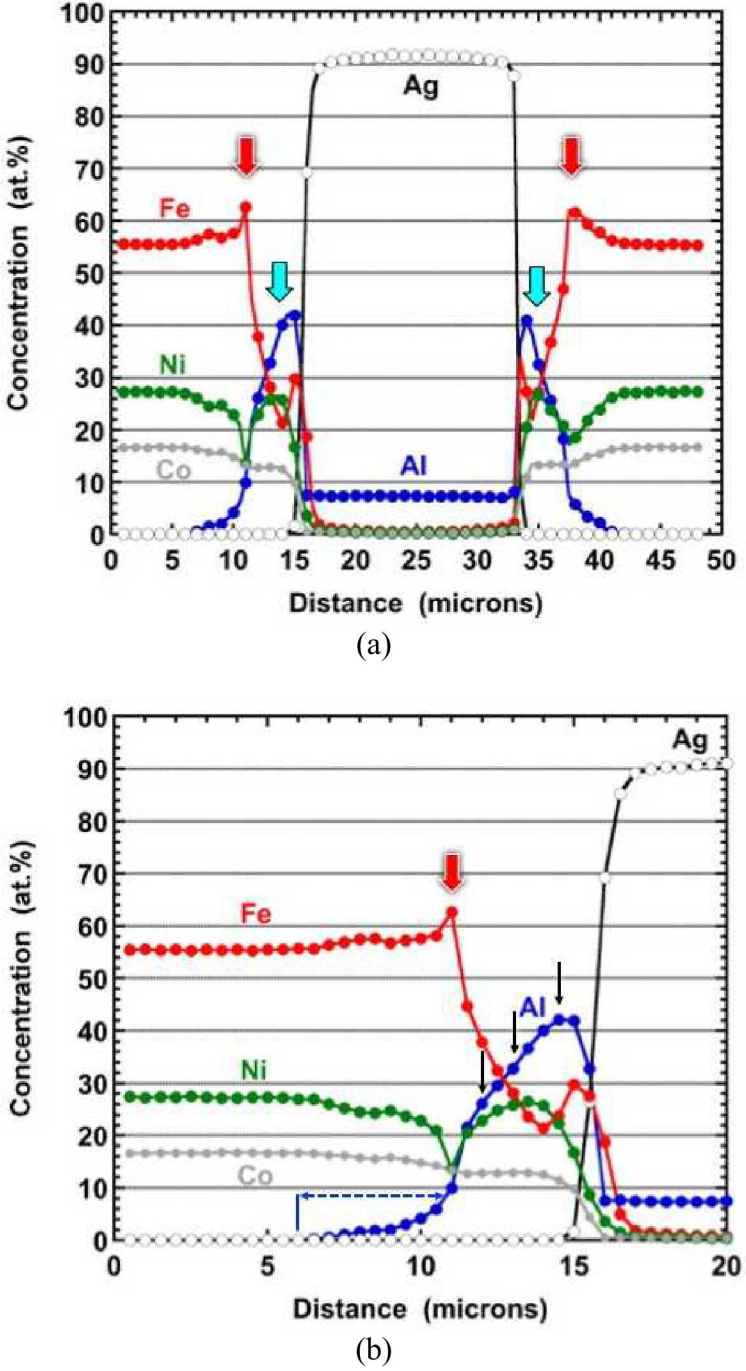


Figure 11 (a) EPMA data obtained from the braze joint fabricated with the Ag-5Al filler metal and brazing conditions of 965°C (1769°F) and 5 min. The red and cyan arrows are the Fe-rich reaction layer and reaction layers, respectively. (b) Enlarged EPMA trace targeted the left-hand side reaction layer. The three black arrows indicate the locations of the low-Al, medium-Al, and high-Al composition calculations. The blue arrow identifies a recrystallization zone.

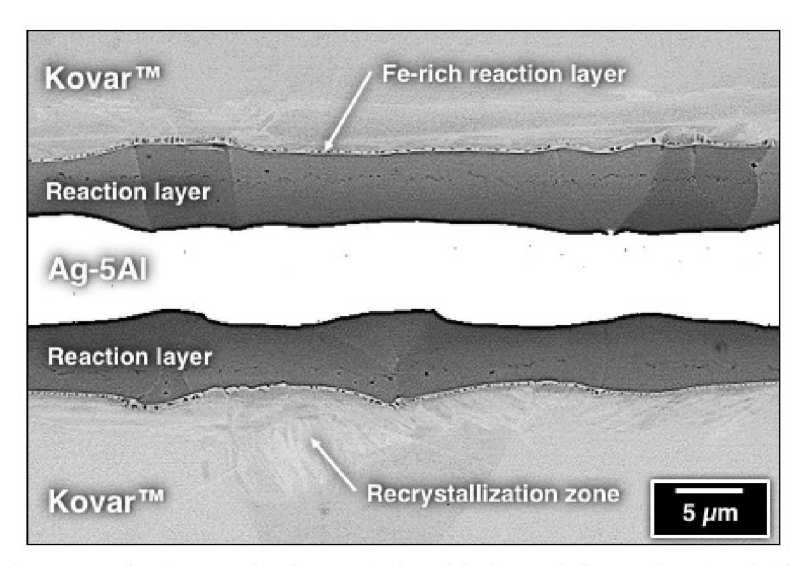


Figure 12 SEM photograph shows the braze joint fabricated from the Ag-5Al filler metal under the brazing conditions of 995°C (1823°F) and 20 min.

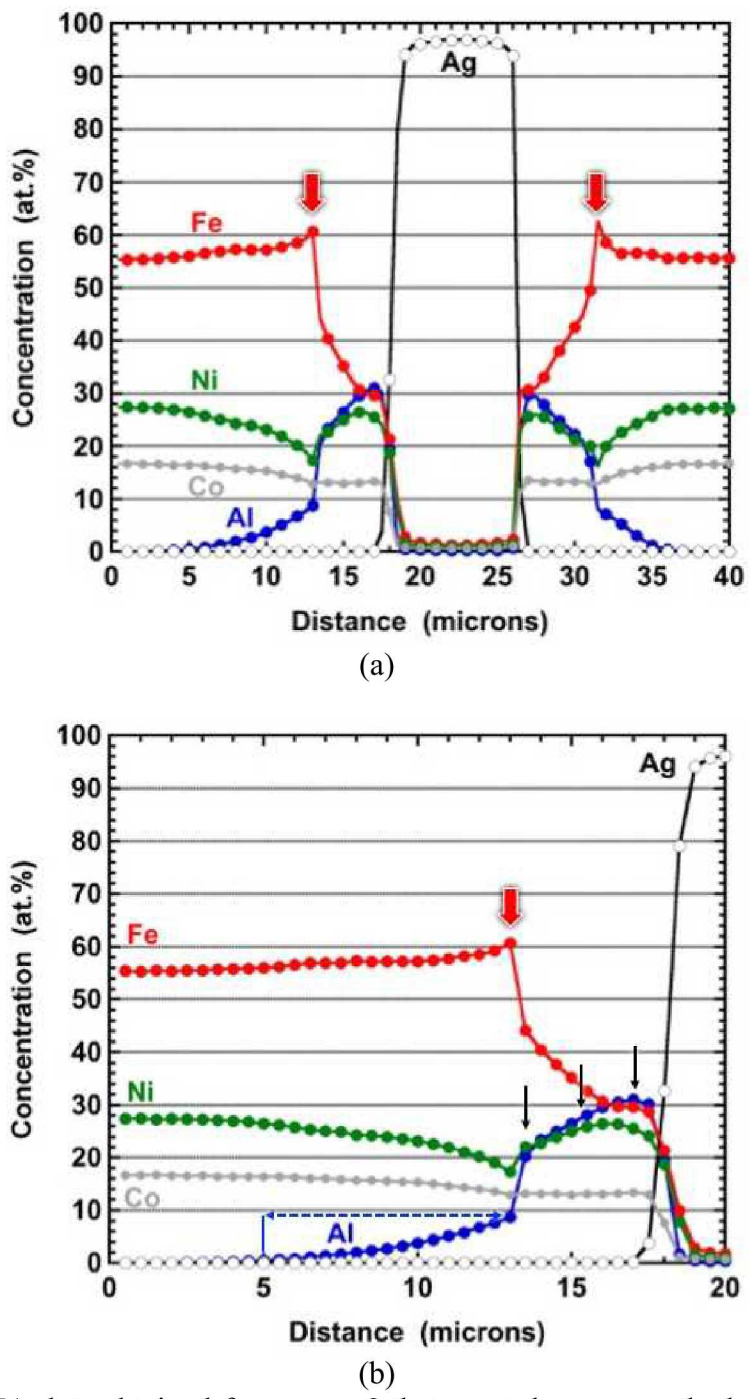
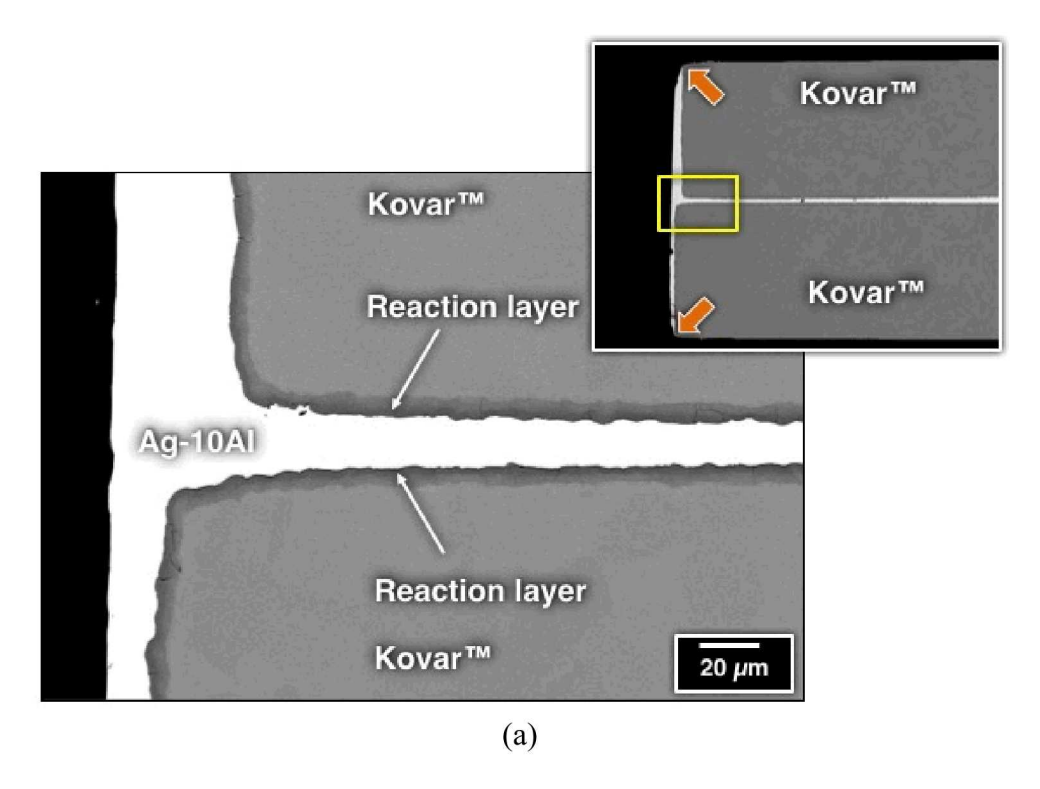


Figure 13 (a) EPMA data obtained from trace 2 that was taken across the braze joint fabricated with the Ag-5Al filler metal and brazing conditions of 995°C (1823°F) and 20 min. The red arrows indicate the Fe-rich reaction layer. (b) Enlarged EPMA trace targeted the left-hand side reaction of trace 2. The three black arrows indicate the locations of the low-Al, medium-Al, and high-Al composition calculations. The blue arrow identifies a recrystallization zone.



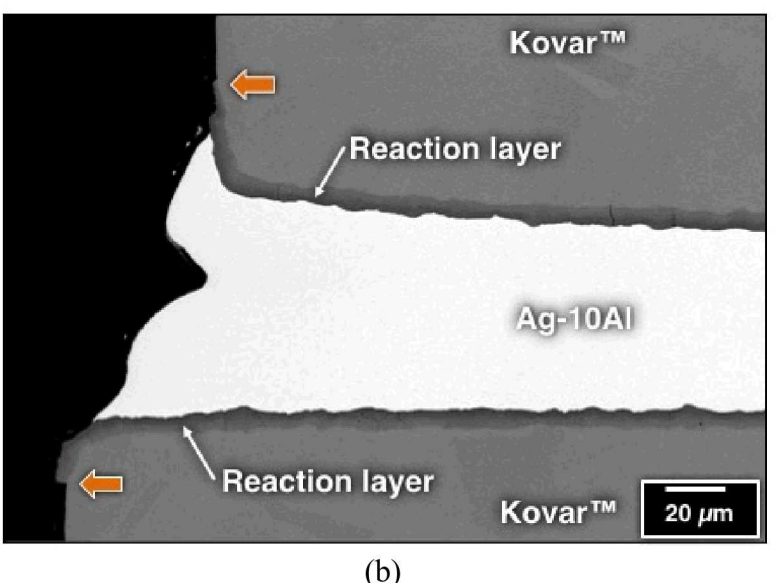
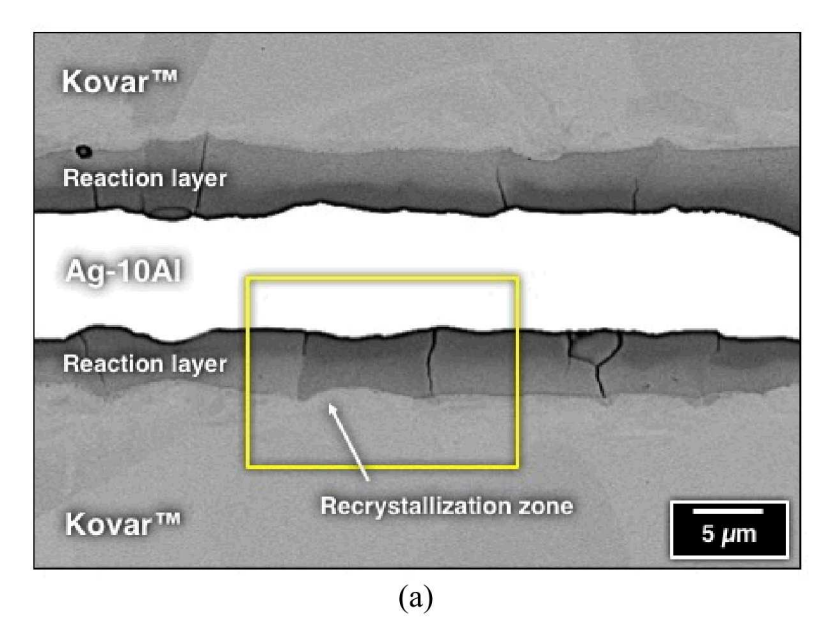


Figure 14 SEM images show the different extents of Ag-10Al wetting and spreading during brazing at 965°C (1769°F) for 5 min. (a) Inset SEM image shows extensive run-out along KovarTM edges to the respective corners (orange arrows). The high magnification photograph shows formation of the reaction layer. (b) SEM image taken of the same braze joint, but at a location where run-out was absent. The orange arrows denote the end of the reaction layers.



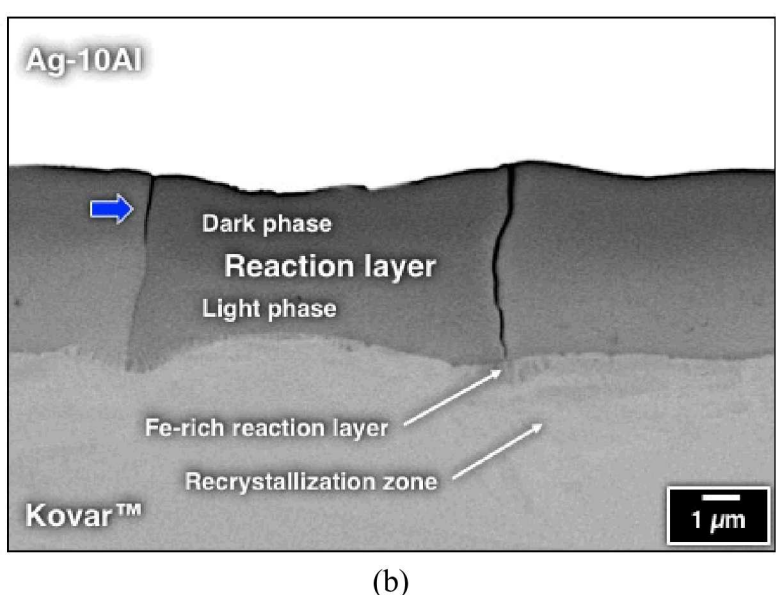


Figure 15 (a) SEM photograph provides a close-up view of the Ag-10Al braze joint microstructure [965°C (1769°F), 5 min]. The yellow box identifies the location of the SEM photograph in (b) that illustrates the microstructure of the reaction layer; the Fe-rich reaction layer; and recrystallization zone. The blue arrow identifies a crack that followed a grain boundary.

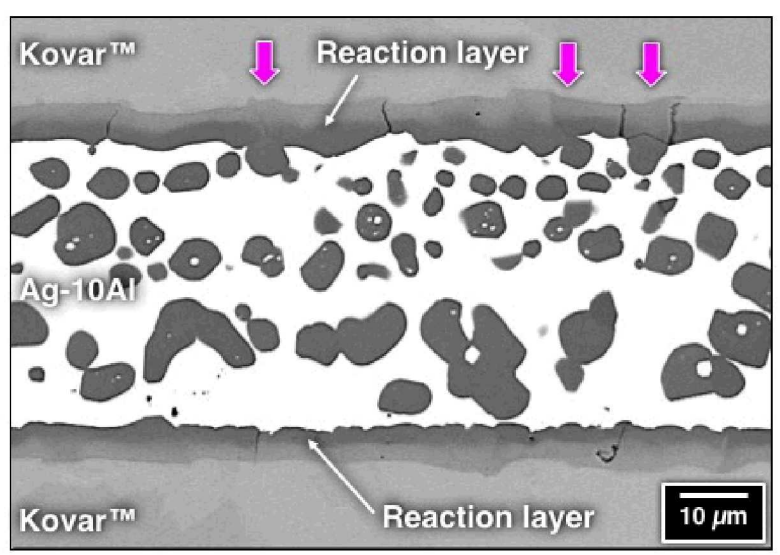


Figure 16 SEM photographs show the cross section of the Ag-10Al braze joint formed at 965°C (1769°F) and 5 min. This location was selected to show a significant particle phase presence in the filler metal. The magenta arrows indicate particles in the process of being formed by spalling from the interface reaction layer.

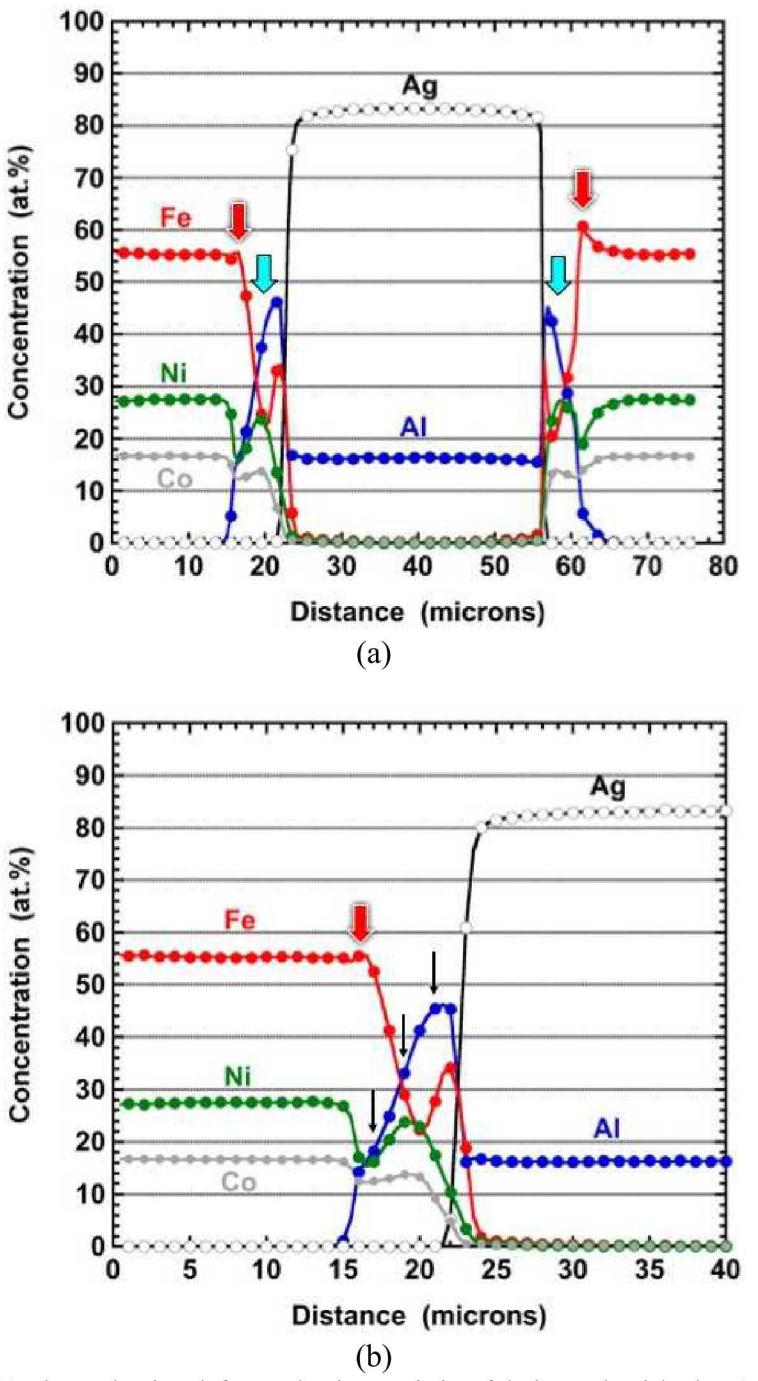
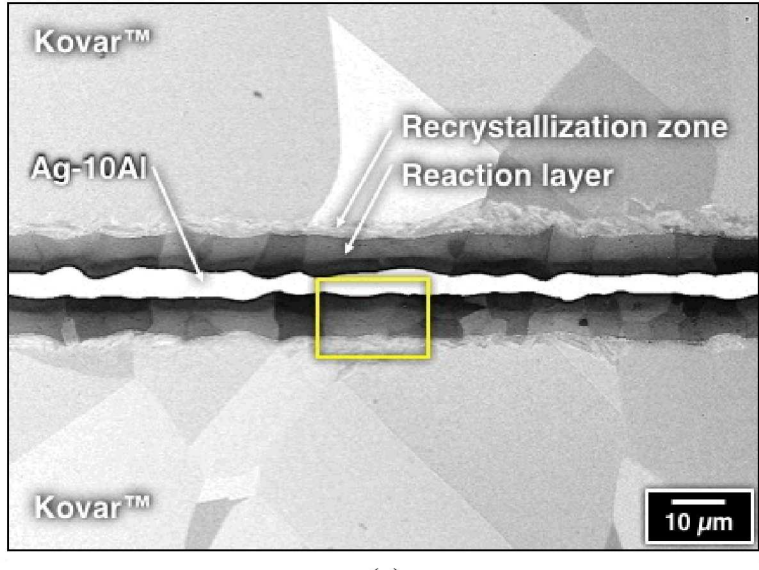
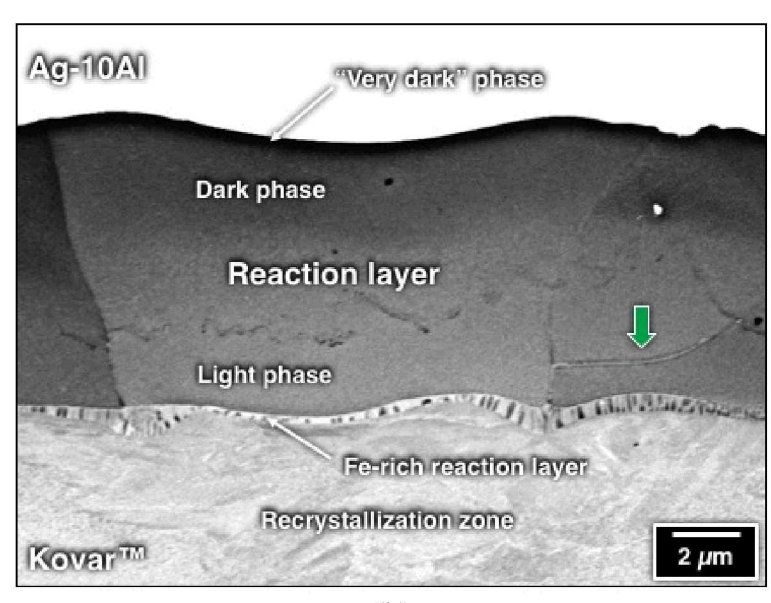


Figure 17 (a) EPMA data obtained from the braze joint fabricated with the Ag-10Al filler metal and brazing conditions of 965°C (1769°F) and 5 min. The red arrows indicated the Fe-rich reaction layers; the cyan arrows identify the Al-bearing, reaction layers. (b) Enlarged EPMA trace shows the left-hand side reaction layer. The black arrows identify the locations where compositions were measured representing low-Al, medium-Al, and high-Al contents.

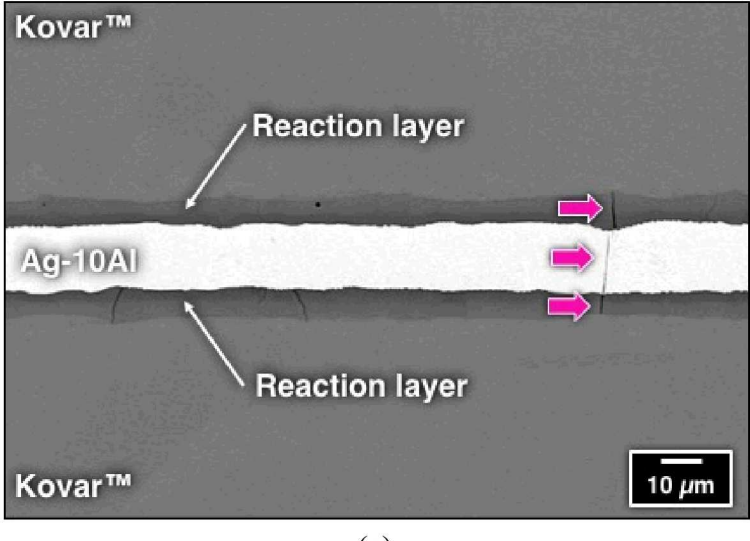


(a)



(b)

Figure 18 (a) SEM photograph the braze joint formed by the Ag-10Al filler metal under the process conditions of 995°C (1823°F) and 20 min. The reaction layers and recrystallization zone are indicated in the image. The yellow box indicates the location of the high magnification photograph in (b). (b) SEM images shows the reaction layer microstructure, including three phases indicated by the gray tone: light, dark, and "very dark". The green arrow indicates a horizontal grain boundary.



(a)

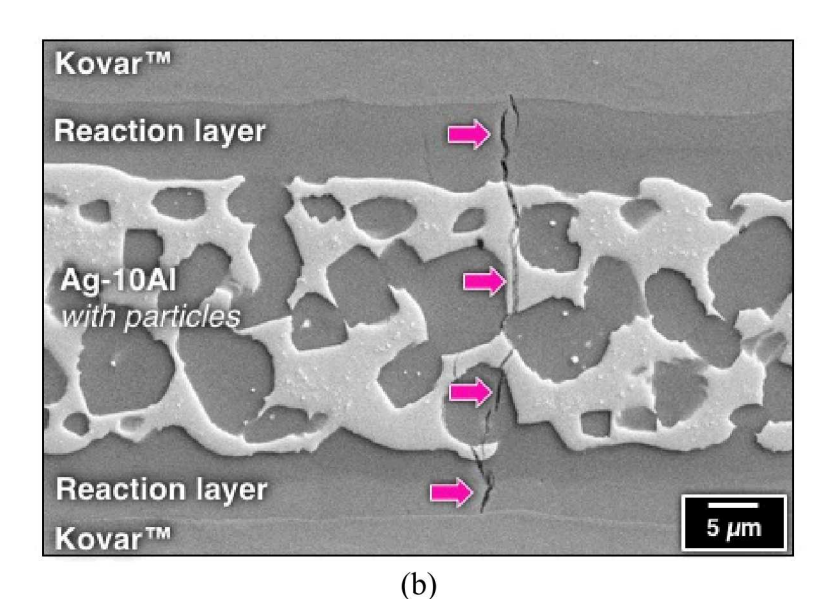


Figure 19 SEM photographs illustrate the development of cracks (magenta arrows) in both the reaction layers as well as across the Ag-10Al filler metal for both microstructures: (a) the absence and (b) the presence of particles in the filler metal. The braze joint was made at 995°C (1823°F) and 20 min.

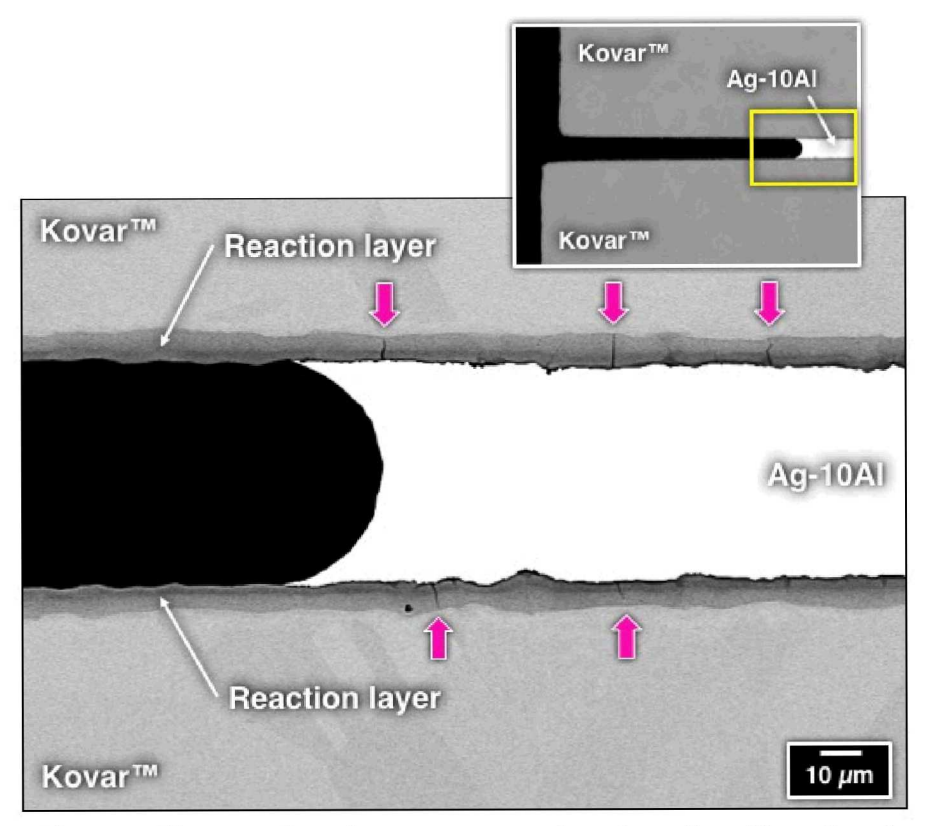


Figure 20 SEM images illustrate the microstructure at the edge of capillary flow by the Ag-10Al filler metal. The inset picture identifies the location (yellow box) with respect to the overall joint configuration. The magenta arrows in the high magnification image point to examples of cracks in the reaction layers. The braze joint was made at 995°C (1823°F) and 20 min.

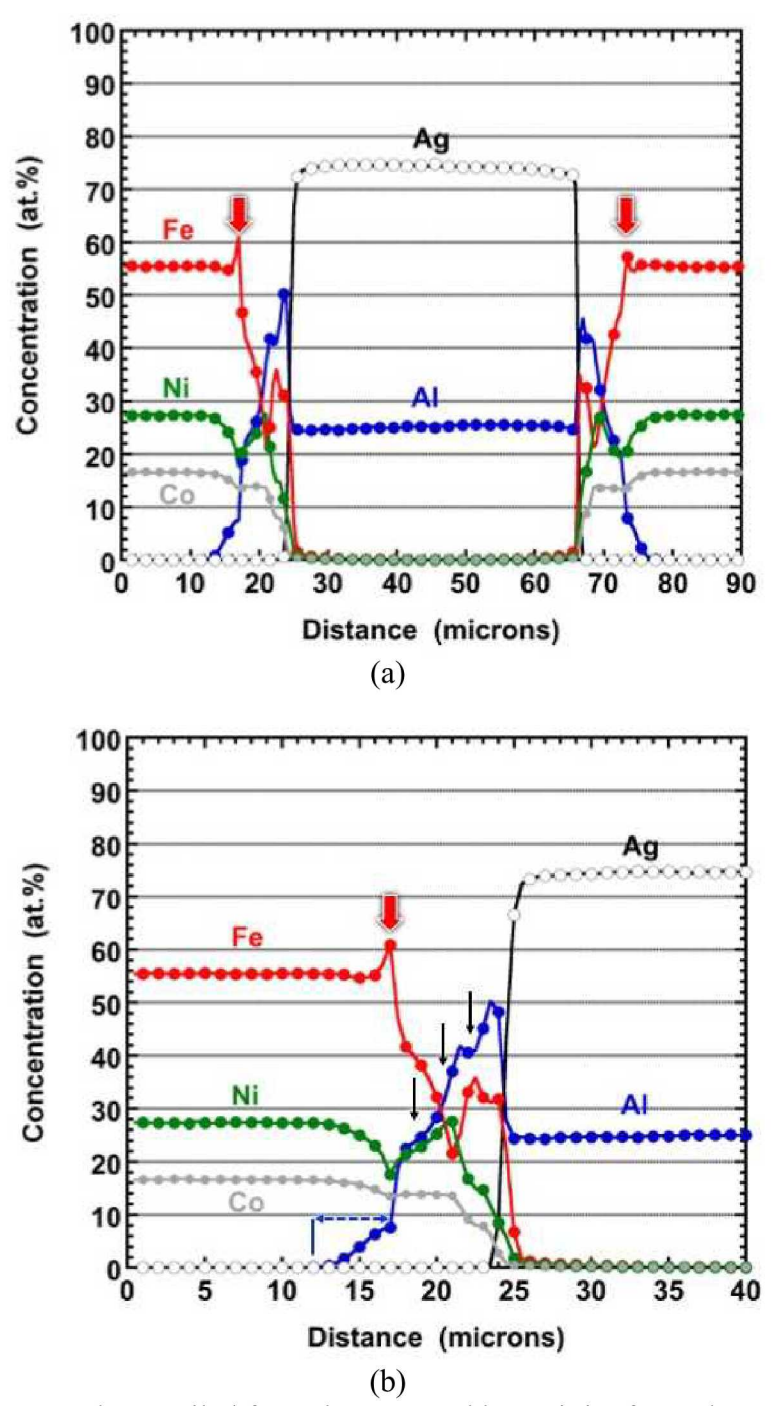


Figure 21 (a) EPMA graph compiled from the Ag-10Al braze joint formed at 995°C (1823°F) and 20 min. The red arrows indicate the Fe-rich layer at the Kovar™ base material / reaction layer interface. (b) Enlarged version of the left-hand side reaction layer in (a). The black arrows indicate the locations at which were established the low-Al, medium-Al, and high-Al phases compositions. The blue arrow shows the extent of the recrystallization zone.

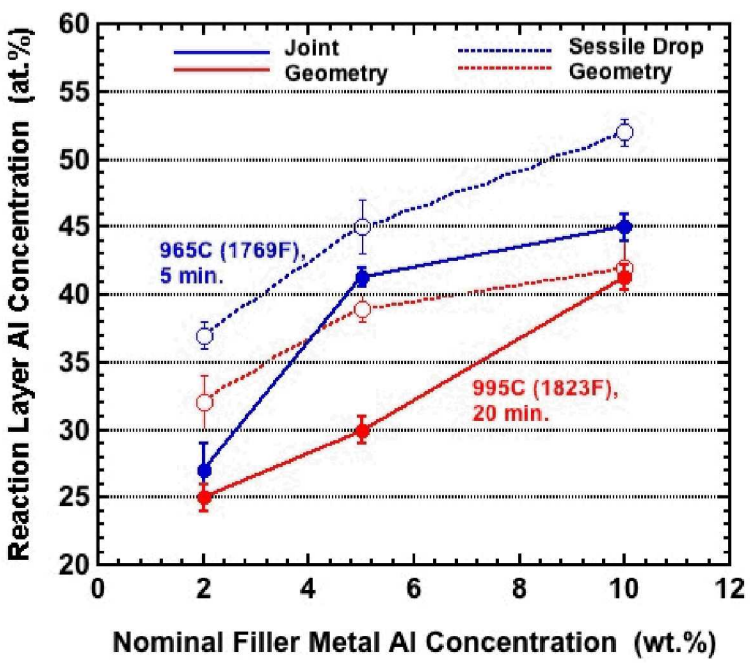


Figure 22 Aluminum concentration (at.%) in the reaction layer contacting the filler metal is plotted as a function of the nominal Al concentration (wt.%) of the filler metal. The blue and red plots show data for the brazing processes of 965°C (1769°F), 5 min and 995°C (1823°F), 20 min, respectively. The closed symbols and solid lines represent the joint configuration; the open symbols and dashed lines represent the sessile drop data from Part 1.

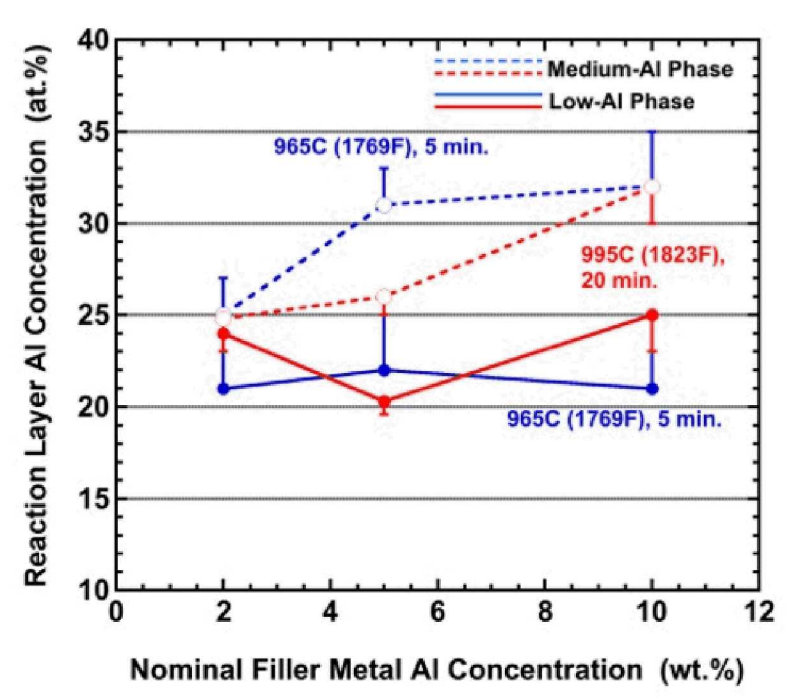


Figure 23 Aluminum concentration (at.%) in the medium-Al (dashed lines) and low-Al (solid lines) reaction layers is plotted as a function of the nominal Al concentration (wt.%) of the filler metal. The blue and red plots represent the brazing processes of 965°C (1769°F), 5 min and 995°C (1823°F), 20 min.

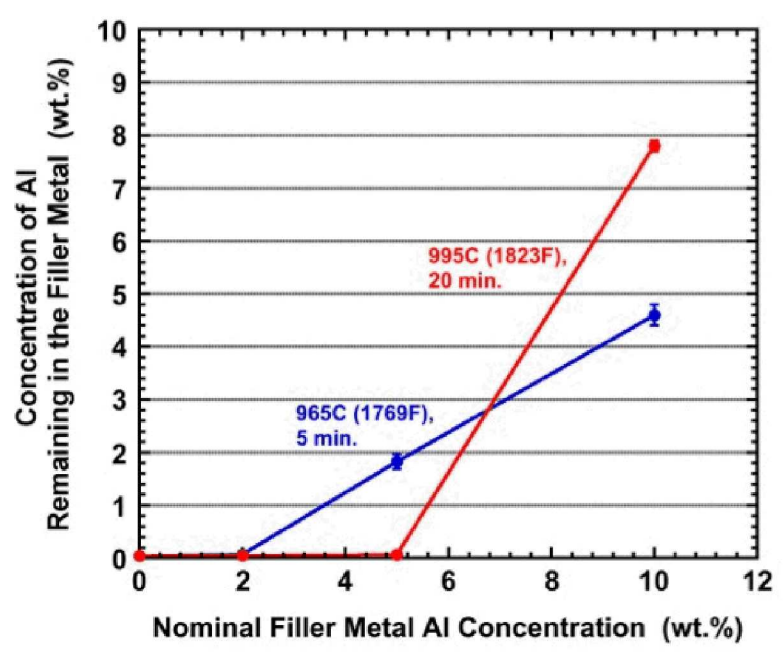


Figure 24 Graph shows the amount of Al remaining in the filler metal as a function of the latter's nominal Al content for the brazing process parameters of 965°C (1769°F), 5 min (blue plot) and 995°C (1823°F), 20 min (red plot).

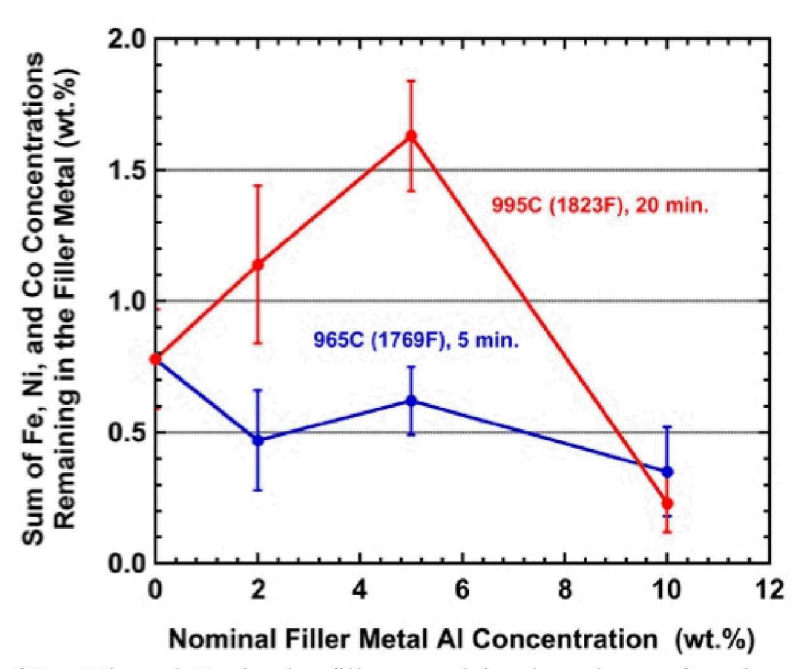


Figure 25 Sum of Fe, Ni, and Co in the filler metal is plotted as a function of the nominal Al content of the filler metal for the brazing process parameters of 965°C (1769°F), 5 min (blue plot) and 995°C (1823°F), 20 min (red plot).

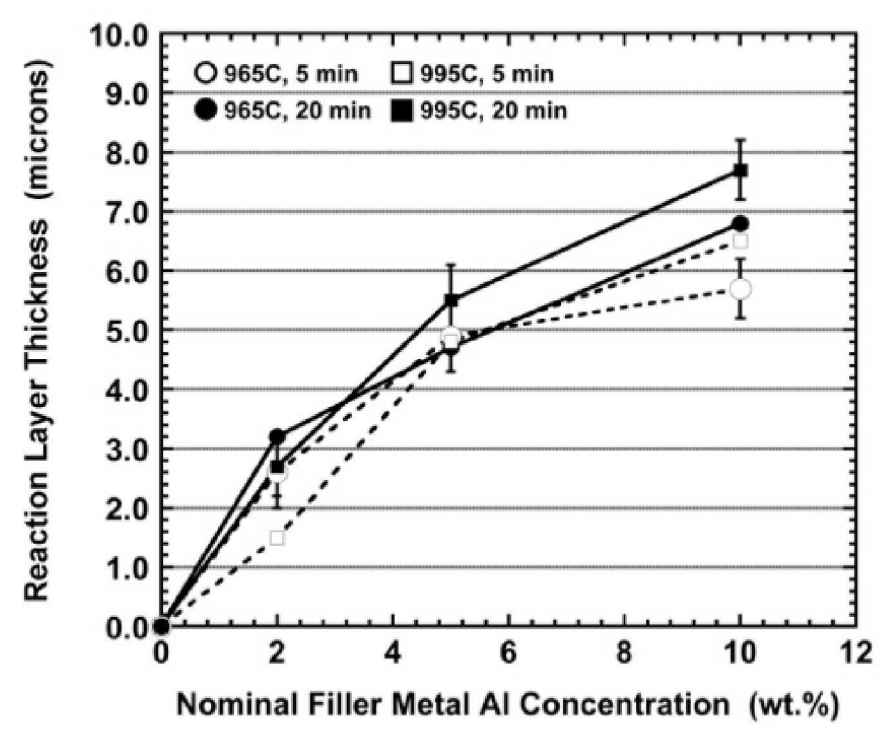


Figure 26 Graph shows the reaction layer thickness as a function of the nominal Al content of the filler metal for all four brazing process conditions used in this study.